# Climate and topographic controls on simulated pasture production in a semiarid Mediterranean watershed with scattered tree cover

**J. Lozano-Parra[1], M. P. Maneta[2] and S. Schnabel[1]**

[1] Geoenvironmental Research Group, University of Extremadura, Avda. Universidad 10071, Cáceres, Spain. jlozano@unex.es; schnabel@unex.es

[2] Geosciences Department, The University of Montana, 32 Campus Drive, Missoula, Montana, USA. marco.maneta@umontana.edu

Correspondence to: J. Lozano-Parra: (jlozano@outlook.es)

## Abstract

Natural grasses in semiarid rangelands constitute an effective protection against soil erosion and degradation, are a source of natural food for livestock and play a critical role in the hydrologic cycle by contributing to the uptake and transpiration of water. However, natural pastures are threatened by land abandonment and the consequent encroachment of shrubs and trees as well as by changing climatic conditions. In spite of their ecological and economic importance, the spatio-temporal variations of pasture production at the decadal to century scales over whole watersheds are poorly known. We used a physically-based, spatially-distributed ecohydrologic model applied to a 99.5 ha semiarid watershed in western Spain to investigate the sensitivity of pasture production to climate variability. The ecohydrologic model was run using a 300 year long synthetic daily climate dataset generated using a stochastic weather generator. The dataset reproduced the range of climatic variations observed under current climate. Results indicated that variation of pasture production largely depended on factors that also determined the availability of soil moisture such as the temporal distribution of precipitation, topography, and tree canopy cover. The latter is negatively

related with production, reflecting the importance of rainfall and light interception, as well as water consumption by trees. Valley bottoms and flat areas in the lower parts of the catchment are characterized by higher pasture production but more interannual variability. A quantitative assessment of the quality of the simulations showed that ecohydrologic models are a valuable tool to investigate long term (century scale) water and energy fluxes, as well as vegetation dynamics, in semiarid rangelands.

## 1. Introduction

Traditional Mediterranean agrosilvopastoral systems support high levels of biodiversity in a wide variety of coexisting natural and man-made habitats, such as grazing areas, agricultural lands, scrublands, forests or wildlife spaces (Joffre et al., 1988;Campos-Palacín, 2004). Natural grasses and pastures are an important element of cohesion between these habitats by supporting livestock and other fauna, by protecting the soil against erosion and degradation, and by controlling the soil hydrologic and thermal regime (Schnabel, 1997;Paço et al., 2009). The economic importance of pasture encourages the proper management and conservation of Mediterranean agrosilvopastoral systems, however owing to climate characteristics of semiarid Mediterranean environments, natural herbaceous production is highly variable with a pronounced seasonality, being highest in spring, low in autumn and winter, and nil during summer (Montero et al., 1998;Joffre and Rambal, 1993). Additionally, pasture yield is usually low and its spatiotemporal distribution is strongly conditioned by the balance of positive and negative effects of limiting factors such as water, light, or nutrients (Brooker et al., 2008).

Decreased pasture yields may upset the balance of habitats and threaten the sustainability of these Mediterranean systems due to changes in land use associated with a revision of economic priorities and management decisions. Indeed, pastures in Mediterranean Europe have been experiencing land abandonment and consequent encroachment of shrubs and forest

(Rivest et al., 2011;García-Ruiz and Lana-Renault, 2011;Lavado-Contador et al., 2004), which may lead to increased competition for resources, such as water and light, among different layers of vegetation (Cubera and Moreno, 2007a). The abandonment of traditional agrosilvopastoral systems may not only have important ecologic consequences but may also have a significant impact on regional economies and on food security by affecting forage quality and quantity and by affecting productivity and protection of the agricultural landscape against degradation.

Improved knowledge of the frequency of low and high pasture productivity periods and the expected variability of yields in different locations of a region permits making better informed management decisions that contribute to the sustainability of agrosilvopastoral systems, however, we still only have a partial understanding of the ecohydrological processes that control plant productivity across space and time (Asbjornsen et al., 2011).

From the mid 90's there has been a growing interest in the complex interactions between ecological and hydrological processes at multiple scales (Viville and Littlewood, 1996;Rodríguez-Iturbe, 2000;Wang et al., 2012;Caylor et al., 2005;Caylor et al., 2009;Porporato et al., 2002;Rodriguez-Iturbe et al., 1999). Because of the complex and non-linear interactions between vegetation and hydrology, few studies focus on the larger scales, such as landscapes or watersheds, where the processes are less understood (Asbjornsen et al., 2011). A limited number of models have been developed in the last decade to investigate ecohydrologic interactions at watershed and regional scales (e.g. Ivanov et al., 2008;Oleson et al., 2010;Tague and Band, 2004;Maneta and Silverman, 2013;Fatichi et al., 2012). Most of the studies using these models have focused on short-term studies because of the long run-times derived from their complexity and because the lack of existing extensive climate data sets (longer than a few decades) needed to force the models. These limitations have resulted in few studies conducting simulations over the entire range of ecohydrological conditions that

can be expected under current climate variability. These studies would be highly valuable to improve our understanding of the variability of pasture production and to inform grassland management.

Reproducing the entire range of ecohydrologic states to capture relevant watershed processes requires the ability to simulate extensive periods in the order of hundreds of years at small spatial (1-50 meters) and temporal (daily) scales. Maneta and Silverman (2013) present a ecohydrologic model with a level of complexity that can make the simulation of extensive periods at detailed spatial and temporal scales tractable while maintaining a strong mechanistic description of the processes. The lack of extensive input datasets to the model can be overcome by producing synthetic datasets with stochastic weather generators (SWG). These tools have been successfully used since the early 80's (Richardson, 1981) to generate long time-series of synthetic weather data that are statistically indistinguishable from observed shorter term climate records (Semenov and Barrow, 2002). SWGs have been used to simulate future scenarios of climate change (Fatichi et al., 2011;Semenov and Barrow, 1997), crop yields (Semenov and Porter, 1995;Ivanov et al., 2007) or regional hydrologic response (Xia, 1996;Dubrovský et al., 2004).

In this paper we use a combination of mechanistic models and SWG to investigate the spatial-temporal variability of pasture production at watershed scales relevant for management. Questions that we seek to address include: How does pasture production respond to climate variability in combination with antecedent basin conditions? How sensitive is the production of pasture to the temporal distribution of precipitation during the year? How important are topographic controls vs climatic controls in determining the spatial and temporal dynamics of production in a watershed? Does the relative importance of these controls vary for different years and under different circumstances?

While abundant studies have applied numerical models to the study of grassland productivity (Montaldo et al., 2005;Istanbulluoglu et al., 2012) and some work has a focus on the spatio-temporal variability of pasture production over long periods (century scale) and large areas (Clark et al., 2003;Tubiello et al., 2007), to the authors' knowledge no studies have applied comprehensive mechanistic numerical models to address the questions posed above. Experimental or field studies have not addressed satisfactorily these questions either because pasture production over large areas is typically determined with a limited number of measurements commonly taken over a few years and at very specific locations (Plaixats et al., 2004;Santamaría et al., 2009). The limited number of samples could provide a skewed or erroneous estimate of the actual long-term pasture production of a region or farm because short term studies with infrequent sampling may not properly capture the effect of weather variations, such as wet and dry periods, and the specific sampling locations may not properly characterize the actual spatial variation. A modeling approach is therefore preferred in this study.

## 2. Study Area

### 2.1. General description

The study area is an experimental drainage basin located in the southwestern part of the Iberian Peninsula with an area of 99.5 ha (Figure 1), characterized by an agrosilvopastoral land use system called *dehesa* in Spain. Geologically, the study area forms part of the Iberian Massif of Precambrian age, being the dominant rocks greywacke and schist, which were eroded giving rise to an erosion surface. Topography of the drainage basin is gently undulating with an average elevation of 394 m asl, being SSW the dominant aspect. Climate is Mediterranean with a high seasonal and inter-annual rainfall variability (Schnabel, 1998), which determines the available water content for plants, and a marked dry season during

125 summer that can last four months or even more. Average annual precipitation for the period
126 between 1999 and 2012 was 488 ± 149.5 mm (mean ± standard deviation) and mean monthly
127 temperatures ranged between 7.4 ± 1.7°C in January to 26.4 ± 1.5°C in July and August.
128 Annual potential evapotranspiration is twice the annual rainfall amount. Vegetation is
129 typically Mediterranean, characterized by a two-layered vegetation structure, with a layer of
130 scattered trees (*Quercus ilex*) at low density (20±18 *individuals* $ha^{-1}$), and a pasture layer.
131 Natural pastures are composed of annual and perennial herbaceous plants, abounding
132 especially annual grasses (such as *Vulpia bromoides*, *Bromus* sp. or *Aira caryophyllea*) and
133 annual legumes (*Ornithopus compressus*, *Lathyrus angulatus* and several species of
134 *Trifolium*), starting to grow with the first rainfall in autumn and reaching maximum
135 production in spring. A layer of shrubs is also frequent (*Retama sphaerocarpa*), commonly
136 eliminated by ranchers to facilitate pasture growth.
137 Soils in the catchment have a high bulk density, ≈ 1.5 g $cm^{-3}$, are poor in nutrients and have
138 low organic matter content: ≈ 3 %, except below tree cover where it is higher in the upper 5
139 cm (Schnabel et al., 2013b). Roots are concentrated in the upper soil layer (Moreno et al.,
140 2005), favoring the higher porosity (≈ 45%) of the topsoil. Two geomorphologic units can be
141 distinguished in the catchment which determines the type of soil and its hydrologic properties.
142 The boundary between these units is marked by the 395 m contour (Figure 1). The
143 geomorphological unit above 395 m is the northern part of the catchment. It constitutes the
144 slopes of a pediment with sandy loam soils classified as Luvisols (FAO, 1988), rich in rock
145 fragments that provides it with a higher permeability and saturated hydraulic conductivity
146 than the remaining soils (Van Schaik et al., 2008;Van Schaik, 2009). Soil depths in this unit
147 are variable, often exceeding 1 m to bedrock and with an argillic B horizon. The other
148 geomorphologic unit, flat to gently undulating, is located in the lower part of the basin. In this
149 unit soils are very shallow (Cambisols and Leptosols), ranging between 20-50 cm, developed

on impervious bedrock of schist and greywacke, which frequently outcrops. The lowest areas of this unit correspond with valley bottoms covered by alluvial sediments reaching a thickness of approximately 1 m in areas next to channels. The main channel is incised into these sediments, actively eroding at present and can be classified as a gully (Gómez-Gutiérrez et al., 2009). Owing to low permeability of these layers some sites are prone to ponding in wet periods (Cerdá et al., 1998;Van Schaik, 2009), which provide an extra water storage that may lengthen the phenological period of the herbaceous plants and that is totally dried in summer. A complete and detailed description of the study area can be found in Maneta (2006) and Van Schaik (2010).

## 3. Methods

### 3.1. Field data

#### 3.1.1 Meteorological data

The study area is equipped with a meteorological station that collects information on precipitation, temperature, relative humidity, global radiation, net radiation, wind speed and direction at intervals of 5 minutes since year 2000. Rainfall is also measured in five other locations (Figure 1) with tipping bucket type rain gauges of 0.2 mm resolution. This information was aggregated in daily intervals for this study.

#### 3.1.2 Soil moisture content and soil temperature

Volumetric soil water content was monitored by capacitive sensors (*Decagon Device, Inc*. model *EC-5*) at 5, 10, 15 and 30 cm depth every 30 minutes. Soil temperature was measured at 5 cm depth near the soil moisture probes (*Decagon Device, Inc*. model *RT-1*). The accuracy of the soil moisture sensors was improved by calibration following the method of Cobos and Chambers (2010). The sensors were grouped in soil moisture stations (SMS) at two sites: *Site*

175 *1* representative of hillslopes with Luvisols, and *Site 2* representative of the lower part of the
176 catchment with shallow soils. A third SMS was installed in the eastern part of the catchment
177 (Figure 1). The selection of sites to install the SMSs were based on previous studies by
178 Lavado-Contador et al. (2006), Maneta *et al.,* (2007, 2008a, b) and Van Schaik *et al*. (2008,
179 2009). The SMSs in *Site 1* and *Site 2* began to register in March 2009, while SMS-3 started in
180 May 2010. In each site there are sensors in open grass areas and under tree canopies. The
181 overall soil moisture of each site was considered to be the depth-averaged soil moisture of the
182 sensors under trees and in open areas, weighted by the relative canopy cover in its pixel.
183

184 ### 3.1.3 Pasture production

185 We have measured natural pasture production at *Site 1* and *Site 2* for three hydrologic years
186 (from Sept 2008 through Aug 2011). To prevent grazing, twelve 1x1 $m^2$ livestock exclusion
187 cages were installed at midslope positions in open space. Only aerial (above-ground)
188 production is considered in this study. Grasses and forbs were cut twice a year (at the end of
189 winter and at the end of spring), dried during 48 hours in an oven at 105°C and weighed to
190 determine aerial dry matter (DM) production (kg DM $ha^{-1}$).
191 Measurements of DM were augmented with measurements of pasture height. At each SMS,
192 16 measurements of plant height were taken biweekly during two hydrological years (from
193 Mar 1, 2011 until Aug 31, 2012). The pasture production database was extended by
194 estimating DM from pasture height measurements using their allometric relationship
195 ($r^2=0.68$, $n=12$).
196

197 ### 3.2. Ecohydrologic model

198 To simulate water and energy exchanges and pasture production we used a spatially
199 distributed ecohydrologic model as described in Maneta and Silverman (2013). This model

couples a two layer (canopy and understory) vertical local closure energy balance scheme, a hydrologic model and a carbon uptake and vegetation growth component. The model was run using climate information from a stochastic weather generator as described below.

Vertical energy transfers are calculated using first-order closure profile equations for momentum, heat and mass under neutral stratification based on flux gradient similarity (Arya, 2001;Foken, 2008). The energy balance is solved for the canopy layer and then for the soil layer using canopy temperature and soil temperature as the closure variables, respectively. Canopy conductance is calculated with a Jarvis-type multiplicative model (Cox et al., 1998;Jarvis, 1976). The model takes into account the vertical and lateral redistribution of water and considers the effect of topography. Water can infiltrate into the soil or become runoff, which can reach the channel and exit the watershed, or re-infiltrate downslope. Water infiltration is calculated using the Green and Ampt approximation to Richard's equation (Chow et al., 1988). Lateral water transfers in the soil are simulated using a 1D kinematic wave model (Singh, 1997). Infiltration and lateral subsurface flows are controlled by soil hydraulic properties (hydraulic conductivity, porosity) and by the topographic gradient. The bedrock at the bottom of the soil is considered to be impermeable and when the soil is fully saturated, return flow occurs. Interception of water by canopies is simulated using a bucket model. The forest growth and carbon uptake components are based on 3-PG (Landsberg and Waring, 1997). See Maneta and Silverman (2013) for further details.

The ecohydrologic model by Maneta and Silverman (2013) was extended in this study with a new grass growth component. Net primary production of grass is related to the available radiation intercepted by the canopy and the water transpired:

$$NPP = C_{NPP} \cdot f(T_a) \cdot \sqrt{\alpha \cdot PAR \cdot \beta \cdot Transp} \quad (1)$$

where *NPP* is net primary production, *PAR* is photosynthetically active radiation intercepted by the canopy, *Transp* is transpiration, $\alpha$ is a constant light use efficiency parameter, $\beta$ is a

constant water use efficiency parameter, $f(T_a)$ is a production efficiency function dependent on air temperature (Landsberg and Waring, 1997), and $C_{NPP}$ is a GPP to NPP conversion factor. Transpiration is calculated from the latent heat term of the energy balance equation for the canopy layer, which takes into account relevant environmental conditions (e.g. air temperature, vapor pressure deficit, soil moisture). Aerodynamic resistance and interception of PAR are related to the leaf area index of vegetation as described in Maneta and Silverman (2013).

The onset of the growing season and the initiation of dormancy are determined by a threshold in the minimum daily air temperature. NPP is allocated to two carbon pools: aboveground biomass (leaves) and belowground biomass (roots). Aboveground biomass is further divided into green aboveground biomass and dead aboveground biomass. The dynamics of these carbon pools are described by three ordinary differential equations that track their mass balance (Montaldo et al., 2005;Istanbulluoglu et al., 2012):

$$\frac{dM_g}{dt} = \phi_a NPP - k_{sg} M_g \tag{2a}$$

$$\frac{dM_r}{dt} = (1-\phi_a) NPP - k_{sr} M_r \tag{2b}$$

$$\frac{dM_d}{dt} = k_{sg} M_g - k_{sd} \xi_{sd} M_d \tag{2c}$$

where $M_g$, $M_r$ and $M_d$ are dry mass in the green grass, root, and dead grass pools, respectively; $k_{sg}$, $k_{sr}$ and $k_{sd}$ are constant decay coefficients for green, root and dead biomass, respectively. Parameter $\xi_{sd}$ is an adjustment factor for the coefficient of dead biomass decay. This adjustment permits to account for reduced decay during the cold season when the temperature of the canopy ($T_c$) drops below a given temperature threshold $T_\xi$:

$$\xi_{sd} = \min\left(1, \frac{T_c}{T_\xi}\right) \quad (3)$$

Parameter $\Phi_a$ (2a, 2b) controls the allocation of NPP to the aboveground (green leaves) and belowground (roots) pool of carbon based on the spare capacity of the land to carry aboveground biomass (Istanbulluoglu et al., 2012) :

$$\phi_a = \left(1 - \frac{LAI_g}{LAI_{\max} - LAI_d}\right) \quad (4)$$

Where $LAI_g$, $LAI_{max}$, and $LAI_d$ are green, maximum, and dead grass leaf area indices, respectively. The denominator of (4) indicates the space available to grow green leaves.

The transformation of the aboveground mass to leaf area index is done using the specific leaf area index for green and dead leaves:

$$LAI_g = \sigma_{LAIg} M_g \quad (5a)$$

$$LAI_d = \sigma_{LAId} M_g \quad (5b)$$

$$LAI_t = LAI_g + LAI_d \quad (5c)$$

Where $\sigma_{LAIg}$ and $\sigma_{LAId}$ are the specific leaf area indices for green and dead leaves. Total leaf area index ($LAI_t$) is considered to be the sum of the green and dead leaf area indices.

## 3.3. Model set up

### 3.3.1 Hydrologic properties, land cover and vegetation parameters

The modeling domain was discretized with a 30 x 30 $m^2$ grid, as used in previous studies (Maneta, Schnabel, & Jetten, 2008). A digital elevation model (DEM) was used to delineate the limits of the basin, obtain a map of local slopes and other basic information on the geometry of the domain. The drainage direction network was calculated using a deterministic

261 steepest descent algorithm (D8 algorithm). Maps of soil properties such as soil depth,
262 porosity, and other hydrologic properties (Figure 2) where derived from the geomorphologic
263 characteristics of the basin as described in Maneta *et al.* (2008). Soil albedo, emissivity and
264 soil thermal capacity were considered uniform in space.
265 Tree density and tree canopy cover maps were obtained manually digitizing a point for each
266 individual tree in a high-resolution aerial photograph, then calculating the density of points
267 using a 3x3 moving average kernel. The fraction of the area covered by canopy was
268 calculated using a maximum likelihood supervised classification technique from a 24-bit
269 color submetric resolution aerial photography. Once a canopy mask was produced, the canopy
270 coverage was obtained by calculating the fraction of pixel classified in each of the larger
271 pixels used in the simulation (Figure 2) (Maneta, 2006). Physiological and structural
272 parameters for trees (*Quercus ilex*) were taken from the literature (Table 1), while parameters
273 related to pasture were mostly manually adjusted (section 3.4).

274

275 ### 3.4. Generation of atmospheric forcing

276 LARS-WG v5.5 (Semenov and Barrow, 2002) is a SWG that generates temporal-series of
277 synthetic weather statistically similar to observations at a single site. LARS-WG generates the
278 synthetic weather by sampling from semi-empirical distributions that takes into account the
279 length and the frequencies of wet and dry periods and the covariance among variables, which
280 is important to properly simulate Mediterranean climates. More information about this SWG
281 can be found in Semenov et al. (1998).
282 We used 13 years of data from our meteorological station (2000-2012) to inform LARS-WG
283 about weather patterns in our basin. We assume that the 13 years of available data are
284 representative of the current climate. Small gaps in the dataset were filled using data from a
285 meteorological station located at a distance of 24 km from the study area. A linear regression

model relating data between the stations was sufficient to correct satisfactorily the differences in the external station. LARS-WG was applied to generate a series of 300 years of minimum and maximum temperature, precipitation and solar radiation at the daily timescale. The generation of a 300 year-long climate dataset was chosen to ensure that we are capturing the most common combinations of weather events and basin antecedent conditions that ranchers are likely to experience during the growing season. Other atmospheric information necessary to run the model was generated as follows: Daily relative humidity was estimated with a multiple regression model that used daily mean, maximum and minimum temperature and daily rainfall as predictors ($r^2$=0.75). Wind velocity was obtained by repeating a series of 51 years extracted from a station located at 24 km from the study site. Daily long wave radiation was estimated from air temperature using the method described by Swinbank (1964).

### 3.5. Model calibration, spin up and data analysis

The calibration runs were done running the period from 1 Sep 2008 to 31 Aug 2012 in a continuous loop using daily time steps. Model parameters listed in Table 2 were manually calibrated until soil moisture, soil temperature and pasture yield achieved steady state and satisfactorily matched the available measurements of soil moisture, soil temperature, and pasture yield based on height measurements. Calibration was based on trial and error systematically changing parameters one at a time. When available, the initial trial value was based on values cited in the literature or based on experience. Model performance was quantified using the coefficient of determination, root mean square error, bias and Nash-Sutcliffe efficiency coefficient between modeled and observed soil moisture, soil temperature and pasture yield. Once performance was satisfactory with parameter values within a realistic range the model was considered calibrated.

The calibrated model was used in a 300 years long simulation at daily time steps resulting in 109500 maps per state variable reported by the model. State variables analyzed included soil moisture, soil temperature, pasture production, pasture evaporation and transpiration, and tree evaporation and transpiration. Time averages and standard deviations for the entire simulation period were calculated for each variable, except for pasture production. For this latter variable, the average and standard deviations for Jun 1$^{st}$ were used in the analysis because this date corresponds to the end of the vegetative period of herbaceous plants and can be considered as the day of maximum accumulated production.

## 4. Results and discussion

### 4.1. Model performance

Mean annual precipitation for the simulated period was 508.8 *mm* with a standard deviation of 118.2 *mm*. Maximum and minimum annual rainfall were 934.1 *mm* and 188.2 *mm*, respectively. The longest dry spell spanned four years with annual rainfalls lower than 386.9 *mm year*$^{-1}$, while the maximum wet period lasted three years with rainfall in excess of 693.4 *mm year*$^{-1}$.

A comparison between simulated and observed atmospheric data indicated that the SWG was properly calibrated and that it successfully generated a synthetic times series that was statistically indistinguishable from the observations (Table 3) except for rainfall in July and August. This is because during these months precipitation volumes are insignificant and small fluctuations about the very low observed precipitation values have a relatively large influence in the K-S statistic. This is of minor importance because rainfall in these months is virtually zero. Further inspection of the results showed that the generated weather series represents the seasonal and inter-annual variations typical of the Mediterranean climate.

An initial inspection of the graphs shown in Figures 3 and 4 indicates that the model reproduced to a high degree the observed dynamic of soil moisture and temperature. The simulation captured the seasonal variations of soil moisture, including the wetting and recession rates, but also much of the observed high-frequency variation. Some mismatch can be observed in the reproduction of wetting peaks, such as those of *Site 1* (Figure 3.A). There is a general dampening of the amplitude of high frequency variations that may be due to the model representation of soil moisture as the average over the entire soil profile (Maneta and Silverman, 2013). However the standard goodness-of-fit statistics and descriptive statistic confirmed a satisfactory fit with high coefficients of determination ($r^2 \geq 0.80$), low RMSE ($\leq$ 0.047 $m^3 m^{-3}$) and similar statistics for all measurement stations (Table 4). Further evaluation of the model performance show high Nash-Sutcliffe coefficients ($\geq 0.75$) and low prediction bias ($\leq 0.018$ $m^3 m^{-3}$).

The simulated soil temperature captured the high-frequency variation of observed soil temperature (Figure 4). However, during the first year simulated temperatures were higher than observed in both study sites, which could be caused by uncommonly low pasture yields simulated that year and hence an overestimation of the amount of radiation reaching the bare soil, while actual ground covered by pasture was much higher at the SMS sites because they were protected against grazing. Efficiency statistics for soil temperature were satisfactory, with coefficients of determination $r^2 \geq 0.89$ and the Nash-Sutcliffe efficiency criterion 0.86, increasing our confidence on the capacity of the model to represent the energy fluxes in the study site (Table 4).

Simulated annual pasture production matched well the observed data at both field sites (Table 4). The average simulated value of production for both sites was 630.9 *kg DM* $ha^{-1}$, very similar to the observed 623.8 *kg DM* $ha^{-1}$. Other descriptive statistics (minimum, maximum, standard deviation) and goodness-of-fit statistics confirming the model in our research area

359 are shown in Table 4. The model produced a satisfactory description of the spatio-temporal
360 dynamics of production, which is supported by the high prediction efficiency of the model
361 (Nash-Sutcliffe $\geq 0.75$; $r^2 \geq 0.76$) and low residual errors (RMSE = 164.8 *kg DM* $ha^{-1}$).
362 The phenological cycle of the herbaceous plants in the study site (Figure 5) is captured in the
363 simulated data and includes low production in autumn although dependent on antecedent
364 precipitation, scarce production in winter because of low air temperatures and available
365 energy, high production in spring when water and energy are available and an absence of
366 production in summer because of lack of water. It is important to note that once pasture is cut
367 at the sites to measure its dry biomass, the exclusion cage is moved to a nearby location,
368 which contributes to the difference between DM estimated from cuts (blue diamonds) and
369 from vegetation height (green circles) since production is highly variable even at short
370 distances (as indicated by the standard deviation of pasture cuts, Figure 5). In contrast, plant
371 height is always and consistently measured at the same location (SMS).
372 Even though we do not have direct measurements of tree transpiration to verify our
373 simulations it is of value to compare our results with the transpiration of *Q. ilex* reported in
374 the literature. Figure 6 shows tree and pasture transpiration during four hydrological years in
375 a pixel of *Site 1* and *Site 2*. Simulated dynamics of tree transpiration in *Site 1* follow a marked
376 seasonal cycle reaching maximum values in spring when environmental conditions were
377 optimal for growth. The maximum simulated value was 1.0 *mm* $d^{-1}$ which is slightly lower
378 than observed values reported by Infante et al. (2003), who measured maximum daily
379 transpiration between 1.2 and 1.4 *mm* $d^{-1}$. Higher values were found by Paço et al. (2009),
380 who even observed values exceeding 2.5*mm* $d^{-1}$. *Q. ilex* maintained transpiration throughout
381 the year, even during summer when the soils are dry.
382 Pasture transpiration is associated with the seasonal phenological cycle typical of annual
383 herbaceous plants. In both sites, low transpiration occurred in autumn and is associated with

low pasture growth (Figure 6). Maximum values were registered in spring, not exceeding 1.75 $mm\ d^{-1}$, when herbaceous plants find the most suitable environmental growth conditions. Similar values were also observed by Paço et al. (2009) in an analogous ecosystem, where the authors estimated maximum peaks in excess of 1.5 $mm\ d^{-1}$, while Joffre and Rambal (1993) found different values depending on the annual rainfall in more humid dehesas, ranging from 2.0 to 2.9 $mm\ d^{-1}$.

## 4.2. Simulations

### 4.2.1. Spatial distribution of soil moisture and evapotranspiration

Simulated average catchment soil moisture for the 300 years was 0.158 $m^3\ m^{-3}$, although strong variations were found among different locations in the study area ranging from 0.070 to 0.285 $m^3 m^{-3}$ (Figure 7.A). Average simulated soil moisture at *Site 1* was slightly lower than at *Site 2*, with 0.174 and 0.201 $m^3\ m^{-3}$, respectively, which is in accordance to the observed differences between sites of measured values (Table 4).

A multiple regression analysis revealed that the most explanatory variables determining the spatial distribution of soil moisture are canopy cover, porosity, slope, and elevation. These variables explained 68% of the observed variance and, with the exception of porosity, showed a negative correlation with soil moisture. Canopy cover showed a particularly strong negative relationship with soil moisture, indicating that the reduction of water reaching the ground due to rainfall interception and the additional water uptake by the trees was a more determinant control of soil moisture than the reduction of incident radiation and evaporation below tree canopies due to shading.

Low lying areas had greater average soil moisture (Figure 7.A). These areas correspond to the valley bottoms and flat footslopes, which show better conditions for water maintenance by the effect of topography (concentrating water) or thicker soils with a higher content of clay and

409 silt particles and greater porosity (McGlynn et al., 2003;Jencso et al., 2009). In contrast,
410 hillslopes and areas at greater altitude had lower soil moisture values, which could be
411 attributed to smaller contributing areas, higher canopy cover and coarser soil textures.
412 However, a small area in the north-eastern upper part of the catchment also showed high
413 average soil moisture values, which could be explained by its low tree density and low canopy
414 cover.
415 These results highlight the importance of trees in the spatial distribution of soil moisture. This
416 has been observed in dehesa systems by Lavado-Contador et al. (2006), Martínez Fernández
417 et al. (2007) or Moreno and Cubera (2008). Whether trees enhance or reduce soil moisture
418 with respect to open areas seems to be dependent on the climatic conditions of the site
419 (Lozano-Parra et al., 2011). Joffre and Rambal (1988) found higher water content beneath tree
420 canopies in sub-humid ecosystems, which could explain enhanced pasture yields in these
421 situations. Likewise, Gindel (1964) observed also higher water content beneath canopy than
422 in open areas under subtropical and semi-desert conditions. In contrast, García-Estringana et
423 al. (2013) measured lower soil moisture under forest cover in a Mediterranean mountain area,
424 while Cubera and Moreno (2007b) and Gea-Izquierdo et al. (2009) found lower water
425 contents beneath canopy in semiarid conditions with scattered trees, which is in accordance
426 with our results.
427 The variability of soil moisture is presented in Figure 7.B and shows a spatial distribution that
428 correlates with the distribution of soil moisture averages. Higher temporal variability of soil
429 moisture was observed in areas with high average soil moisture (e.g. valley bottoms). In
430 contrast, areas with low mean soil water content such as hillslopes with high gradients
431 showed less temporal moisture variability. An explanation for this behavior is that regions
432 with intermediate and higher water contents and soils with good retention properties have

more opportunities for soil moisture fluctuations than drier soils with poorer soil water retention capabilities that quickly drain and dry.

Simulated evapotranspiration was marked by the spatial distribution of vegetation cover and by topography (Figure 7.C). Maximum values were found in the valley bottoms where water content remained high during most of the year. High values were also observed in areas with high tree density, while they were lower in open areas where herbaceous vegetation dominates. Annual mean value of actual evapotranspiration for the whole catchment was 390 *mm* while annual mean precipitation was 508 *mm*. This implies that about 120 *mm* could become runoff or to be stored in the soil reservoirs (Figure 1) or rock fractures of the impermeable bedrock of the catchment. In support of this, Schnabel et al. (2013a) measured in the same environment runoff values that oscillated between 10 and 190 *mm* depending on annual precipitation. The simulated annual evapotranspiration values in areas of relatively high tree density are similar to the 590 *mm* reported by Joffre and Rambal (1993) under tree cover in sub-humid Mediterranean rangelands. They found, however, higher annual values, 400 *mm*, in open spaces, which could be explained because their study was carried out in a wetter environment.

### 4. 2.2. Pasture production: temporal dynamics

At *Site 1* annual average dry matter production was 338.0 $kg\ ha^{-1}$, with a standard deviation of 172.5 $kg\ ha^{-1}$, and maximum and minimum values of 977.6 and 20.7 $kg\ ha^{-1}year^{-1}$, respectively (Table 5). At *Site 2* annual average dry matter production was higher (456.0 $kg\ ha^{-1}$), also with higher maximum (1030.9 $kg\ ha^{-1}year^{-1}$) and minimum (29.9 $kg\ ha^{-1}year^{-1}$) values of annual dry matter production. *Site 1* showed higher relative variation of production as compared to *Site 2*. Coefficients of variation for each site were 0.51 and 0.40, respectively.

Also, the range of pasture production was slightly higher at *Site 2* (approximately 1000 *kg DM* $ha^{-1}year^{-1}$ compared to 957 *kg DM* $ha^{-1}year^{-1}$ for *Site 1*). These production values rank the study site as a low productivity rangeland that requires the introduction of supplementary fodder to maintain livestock. Bell (2006) reports that the critical pasture mass necessary to sustain a sheep ranch is between 400 and 1700 *kg DM* $ha^{-1}$, while for cattle 700 to 2900 *kg DM* $ha^{-1}$. Productivity values for similar Mediterranean rangelands are highly variable, as reported by González et al. (2012) with productions that oscillated between 200 and 6372 *kg DM* $ha^{-1}year^{-1}$ in diverse rangelands with a wide range of variations in climate, livestock density and pasture improvements with fertilizations. Gómez Gutiérrez and Luis Calabuig (1992) studied several kinds of grasslands with scattered tree cover, determining annual productions lower than 500 *kg DM* $ha^{-1}$ in many areas.

Plant growth depends on soil water availability that, in turn, is influenced by rainfall variations (Schnabel, 1997). Houérou and Hoste (1977) and González et al. (2012) found that the annual distribution as well as the interannual variations of precipitation had a significant influence in the correlation between precipitation and pasture production. The effect of rainfall variations on simulated pasture production for *Site 1* and *Site 2* are shown in Figures 8 and 9, respectively. The graphs show annual pasture production over 300 years along with a 10-year window of results at the daily timescale that reflect the annual distribution of production. Annual pasture yield depended on annual rainfall amounts and the seasonal distribution, with periods of less yield corresponding to drier years, and greater productions in wetter years.

The seasonal distribution of rainfall did also influence pasture production. Accumulated antecedent precipitation before June was a good predictor of the yield regardless of the total annual precipitation. Years with low accumulated precipitation before June were less producitive than years with higher accumulated precipitation (Table 6). For example, similar

482 annual rainfall occurred in years 210 and 213, however in the year 213 the rainfall of the last
483 four months prior to June was higher, which resulted in a greater yield. In the year 215 a large
484 amount of rainfall occurred after May, but pasture production that year was low.
485 Antecedent rainfall of the last 120 days before June was the variable that explained best the
486 annual pasture production ($r^2$ = 0.73 and $r^2$ = 0.51, for *Site 1* and *Site 2*, respectively). Shorter
487 accumulation periods for antecedent precipitation had poorer correlations with yield, which
488 can be explained because they are associated with less growing time and because as summer
489 approaches there is an increase in evaporation losses.
490

491 **4. 2.3. Pasture production: spatial distribution**

492 The spatial distribution of simulated pasture production varied greatly across the basin. Figure
493 10.A presents the spatial distribution of average production in the catchment over the entire
494 300 simulated years. Areas of higher production tended to have higher variability in their
495 production (Figure 10.B) as well as higher maximum and minimum productivities (Figure
496 10.C and Figure 10.D). Productivity areas were persistent in time, with distributions
497 determined by physiographic characteristics of the basin and the distribution of trees. A
498 multiple regression analysis of pasture production with different variables showed that soil
499 moisture, slopes, tree density, canopy cover, and upslope catchment area were the best
500 predictors of production ($r^2$ = 0.81).
501 The distribution, composition and structure of plant communities are directly conditioned by
502 spatio-temporal patterns in water availability (Asbjornsen et al., 2011) which is strongly
503 determined by topography. In the study catchment the spatial distribution of the natural
504 pastures was clearly influenced by the distribution of soil moisture. Areas with higher water
505 availability had greater yield (Figure 11.A). Low yields were obtained if average soil moisture
506 was lower than 0.150 $m^3\ m^{-3}$. Slope also played a strong role in the distribution of yield.

507 Topographically, valley bottoms and flat areas of the catchment were characterized by higher
508 pasture production. Production decreased rapidly as slope increased (Figure 11.B). This is
509 because in semiarid regions higher slopes are associated with reduced infiltration, enhanced
510 drainage and production of overland flow (Cerdá et al., 1998). The importance of
511 physiographic controls on soil moisture distribution and hence of pasture production in the
512 study region was clearly documented in Ceballos-Barbancho and Schnabel (1998) and Van
513 Schaik (2009), who demonstrated the importance of soils in low lying areas as water storages
514 and the fundamentally different hydrologic regimes of hilltops, hillslopes, low areas and
515 valley bottoms.
516 Canopy cover exerted a strong control on pasture yield (Fig 11.C). An initial explanation is
517 that pixels with high canopy coverage have higher interception of incident precipitation, more
518 transpiration and therefore reduced soil moisture. This interpretation is however insufficient
519 since the influence of trees on pasture production is a more complex issue that involves a
520 number of processes not explicitly simulated in this study. For instance, trees may promote
521 pasture production by enhancing soil fertility and structure or by providing a shaded and
522 favorable microclimate. These factors were not explicitly simulated in this study. Still, it is
523 known that in semiarid ecosystems, rainfall interception together with soil water uptake by
524 trees in areas of high canopy cover would increase the competition for water resources
525 between trees and pastures rather than enhance the productivity of pastures (Moreno, 2008).
526 However, because the model used in this study does not incorporate many processes
527 describing the overstory-pasture relationships such as the effect of vegetation on nutrients and
528 on the soil microbial activity, we cannot conclude that tree canopy cover is strictly
529 detrimental to the productivity of pastures. Indeed, several studies in the region show
530 increased yield under trees as compared to open areas (Moreno, 2008). It has been observed
531 that moderation of incident light could have a positive effect on crop productivity by altering

the microclimate under trees, however this effect depends on antecedent conditions and the production of previous years (Gea-Izquierdo et al., 2009). Values of 13% of canopy cover with 24 *trees* $ha^{-1}$ were considered optimum for understory pasture production (Montero et al., 2008).

### 4. 2.4. Climatic and physiographic factors

The degree to which the various controls discussed in the previous sections determine the distribution of pasture is not invariant. Precipitation is a main driver of total production (Fig 12.A) in almost a linear fashion, but the spatial distribution of pasture is to a large extent controlled by topography, since the spatial variability of precipitation in the study area is very small. In Fig 12.A we distinguish between low, medium, and high production years. These years are clearly related to total precipitation amounts during the February-June period (50 mm to 150 mm of precipitation are associated with years of low production, 150 to 250 mm correspond to years of medium production and more than 250 mm yields high production). Rainfall is related to pasture growth through an associated increase in soil moisture available for uptake. While precipitation is related to production in a somewhat linear relationship, soil moisture is related to pasture productivity in a nonlinear, approximately sigmoidal relationship (Figure 12.B) that starts to reveal the effects of the heterogeneity of the terrain. Figure 12.B suggests that the precipitation amounts only have a scaling effect on the relationship between soil moisture and pasture production. The functional form of this relationship or the ability of soil moisture to explain pasture production remains relatively unchanged.

Unlike rainfall, the distribution of soil moisture is affected by the heterogeneity of the terrain, but the strength of this effect is proportional to the amount of soil moisture, which is partially controlled by the amount of precipitation. For instance low local slopes drive soil moisture by

reducing flow velocity and by increasing the opportunity for infiltration, therefore high production tends to be found in flatter areas of the terrain (Fig 12.C). The effect of the slope, though, is stronger during wetter years when soil moisture is higher and there is more opportunity for overland and subsurface redistribution of water. For drier years the ability of the local slope to explain the spatial variance of production decreases (Fig 12.C).

The relative position of a location in the drainage network, as defined by its upstream catchment area, is a non-local topographic control that also has a strong role in explaining the distribution of pasture production. More water is potentially drained at locations with a larger upstream catchment area, making them more prone to have a higher soil moisture content. Indeed, the productivity of a location increases with its upstream catchment area (Fig 12.D). Local drainage is defined by the small scale topographic features of the surface that form a convergent network. During years of low precipitation, concentration of moisture in converging areas of the drainage network produces a very contrasting spatial distribution of pasture production. The strength of this topographic control during dry years can be assessed by its relatively high explanatory power of the total spatial variance of pasture production. For increasingly wetter years, the strength of this topographic control wanes and with it its explanatory power (Fig 12.D). The contribution of upstream inflows to total local soil moisture decreases as incident precipitation increases. This reduces the influence of the non-local topographic controls.

Overall, during years of abundant production of pasture the importance of upstream water inflows tend to be overwhelmed by relatively large inputs of precipitation. In these conditions local topographic controls such as low slopes that reduce local water drainage rates have a relatively higher influence in the observed pasture productivity. As precipitation inputs are reduced the importance of the lateral redistribution of water becomes more relevant and non-

581 local controls such as the upstream drainage area becomes increasingly more explanatory of
582 the distribution of pasture.
583
584 ## 5. Conclusions
585 Ecohydrological spatially-distributed models in conjunction with statistical weather
586 generators are effective tools for simulating long-term pasture production dynamics and
587 hydrologic conditions in semiarid rangelands, characterized by high spatial and temporal
588 climatic and hydrologic variability. Results from this study contribute to insight into the
589 hydrologic and climatic controls that determine the spatial and temporal distribution of
590 grasses and the expected range of pasture production in different areas at the watershed scale.
591 This study aims at informing rangeland management and promoting the sustainability of
592 grasslands. Spatially, the general physiographic characteristics of the terrain are good
593 predictors of pasture yield, but the distribution of the canopy overstory is also important.
594 Valley bottoms and flat areas adjacent to slopes, which tend to have relatively high soil
595 moisture contents, had the highest production in the study area. Tree canopy cover was found
596 to be negatively related with pasture production, reflecting the importance of rainfall and light
597 interception, as well as water consumption by trees, in the development of a grassy understory
598 in semiarid rangelands.
599 The simulated pasture production in the study catchment ranged from 21 $kg\ ha^{-1}year^{-1}$ to
600 1030.9 $kg\ ha^{-1}year^{-1}$, which ranks it as a medium to low productivity compared to other
601 Mediterranean rangelands. With the calculated yields, the introduction of supplemental fodder
602 is necessary to maintain livestock. Although the interannual distribution of precipitation is a
603 strong control on the variability of pasture yield, its seasonal distribution during the year is as
604 important. Specifically, years with low rainfall from February to May showed limited yield
605 even for years with relatively high annual precipitation.

606 The importance of topographic controls, as captured by the accumulated drainage area,
607 becomes more relevant to explain the spatial distribution of pasture during years of low
608 precipitation. This is because water inflows associated with lateral redistribution processes
609 become a larger proportion of the total inflow into a location due to reduced precipitation
610 inputs. The influence of lateral redistributions of water and therefore of the topographic
611 structure of the watershed is reduced as spring precipitation inputs increase.
612 Although the model used in this study showed good performance in the simulation of water
613 and vegetation dynamics in the study region and therefore provide confidence that the first
614 order controls are captured, important processes, believed to play an important role in the
615 long-term dynamics of pasture production, were not explicitly simulated. An example of these
616 processes is the feedback between climatologic, ecohydrologic processes and the cycling of
617 nutrients.
618
619
620 **Acknowledgements**
621 Research was financed by the Spanish Ministry of Education and Science through projects
622 CGL2008-01215, CGL2011-23361 and the pre-doctoral grant BES-2009-011964. Dr
623 Maneta's contribution to this work was partially supported by the National Science
624 Foundation EPSCoR Cooperative Agreement #EPS-1101342 and the MSGC contract G226-
625 10-W1749. The authors acknowledge the advice received by Professor Anna Sala of the
626 Division of Biological Sciences of The University of Montana, as well as by members of the
627 Geoenvironmental Research Group.
628
629
630 **References**

631 Arya, S. P.: Introduction to micrometeorology, Academic Press, San Diego, CA, 2001.
632 Asbjornsen, H., Goldsmith, G. R., Alvarado-Barrientos, M. S., Rebel, K., Osch, F. P. V., Rietkerk, M.,
633 Chen, J., Gotsch, S., Tobón, C., Geissert, D. R., Gómez-Tagle, A., Vache, K., and Dawson, T. E.:
634 Ecohydrological advances and applications in plant–water relations research: a review, Journal of
635 Plant Ecology, 4, 3-22, 10.1093/jpe/rtr005, 2011.
636 Barboutis, J. A., and Philippou, J. L.: Evergreen Mediterranean hardwoods as particleboard raw
637 material, Building and Environment, 42, 1183–1187, 10.1016/j.buildenv.2005.07.053, 2007.
638 Bell, A.: Pasture assessment and livestock production, in, Primary Industries Agriculture. NSW
639 Department of Primary Industries, State of New South Wales, Australia, http://www.dpi.nsw.gov.au,
640 2006.
641 Brooker, R. W., Maestre, F. T., Callaway, R. M., Lortie, C. L., Cavieres, L. A., Kunstler, G., Liancourt, P.,
642 Tielbörger, K., Travis, J. M. J., Anthelme, F., Armas, C., Coll, L., Corcket, E., Delzon, S., Forey, E.,
643 Kikvidze, Z., Olofsson, J., Pugnaire, F., Quiroz, C. L., Saccone, P., Schiffers, K., Seifan, M., Touzard, B.,
644 and Michalet, R.: Facilitation in plant communities: the past, the present, and the future, Journal of
645 Ecology, 96, 18-34, DOI: 10.1111/j.1365-2745.2007.01295.x, 2008.
646 Campos-Palacín, P.: Towards a sustainable global economics approach for Mediterranean
647 agroforestry systems, in: Sustainability of agrosilvopastoral systems -Dehesas, Montados-. Advances
648 in Geoecology, edited by: Schnabel, S., and Ferreira, A., Catena Verlag, Reiskirchen, Germany, 13-28,
649 2004.
650 Caylor, K. K., Manfreda, S., and Rodriguez-Iturbe, I.: On the coupled geomorphological and
651 ecohydrological organization of river basins, Advances in Water Resources, 28, 69-86,
652 10.1016/j.advwatres.2004.08.013, 2005.
653 Caylor, K. K., Scanlon, T. M., and Rodriguez-Iturbe, I.: Ecohydrological optimization of pattern and
654 processes in water-limited ecosystems: A trade-off-based hypothesis, Water Resour. Res., 45,
655 W08407, 10.1029/2008wr007230, 2009.
656 Ceballos-Barbancho, A., and Schnabel, S.: Hydrological behaviour of a small catchment in the *dehesa*
657 landuse system (Extremadura, SW Spain), Journal of Hydrology, 210, 146-160, 10.1016/S0022-
658 1694(98)00180-2, 1998.
659 Cerdá, A., Schnabel, S., Ceballos, A., and Gómez-Amelia, D.: Soil hydrological response under
660 simulated rainfall in the dehesa land system (Extremadura, SW Spain) under drought conditions,
661 Earth Surface Processes and Landforms, 23, 195-209, 10.1002/(SICI)1096-
662 9837(199803)23:3<195::AID-ESP830>3.0.CO;2-I, 1998.
663 Chow, V. T., Maidment, D. R., and Mays, L. W.: Applied hydrology, McGraw-Hill, New York, xiii, 572
664 pp., 1988.
665 Clark, S. G., Austen, E. A., Prance, T., and Ball, P. D.: Climate variability effects on simulated pasture
666 and animal production in the perennial pasture zone of south-eastern Australia.1. Between year
667 variability in pasture and animal production, Australian Journal of Experimental Agriculture, 43, 1211-
668 1219, 10.1071/EA02101, 2003.
669 Cobos, D. R., and Chambers, C.: Calibrating ECH2O Soil Moisture Sensors. Decagon Device.
670 Application Note, in, www.decagon.com, 2010.
671 Cox, P. M., Huntingford, C., and Harding, R. J.: A canopy conductance and photosynthesis model for
672 use in a GCM land surface scheme, Journal of Hydrology, 212-213, 79-94, 10.1016/S0022-
673 1694(98)00203-0, 1998.
674 Cox, P. M., Betts, R. A., Bunton, C. B., Essery, R. L. H., Rowntree, P. R., and Smith, J.: The impact of
675 new land surface physics on the GCM simulation of climate and climate sensitivity, Climate Dynamics,
676 15, 183-203, 10.1007/s003820050276, 1999.
677 Cubera, E., and Moreno, G.: Effect of land use on soil water dynamic in dehesas of Central-Western
678 Spain, Catena, 71, 298-308, 10.1016/j.catena.2007.01.005, 2007a.
679 Cubera, E., and Moreno, G.: Effect of single *Quercus ilex* trees upon spatial and seasonal changes in
680 soil water content in dehesas of central western Spain, Annals of Forest Science, 64, 355-364,
681 10.1051/forest:2007012, 2007b.
682

683 Dubrovský, M., Buchtele, J., and Žalud, Z.: High-frequency and low-frequency variability in stochastic
684 daily weather generator and its effect on agricultural and hydrologic modelling, Climate Change, 63,
685 DOI: 10.1023/B:CLIM.0000018504.99914.60, 2004.
686 FAO: FAO-UNESCO soil map of the World. Technical report 60., FAO, Rome, 1988.
687 Fatichi, S., Ivanov, V. Y., and Caporali, E.: Simulation of future climate scenarios with a weather
688 generator, Advances in Water Resources, 34, 448-467, 10.1016/j.advwatres.2010.12.013, 2011.
689 Fatichi, S., Ivanov, V. Y., and Caporali, E.: A mechanistic ecohydrological model to investigate complex
690 interactions in cold and warm water-controlled environments: 1. Theoretical framework and plot-
691 scale analysis, Journal of Advances in Modeling Earth Systems, 4, M05002, 10.1029/2011MS000086,
692 2012.
693 Foken, T.: Micrometeorology, Springer, Berlin, xix, 306 p. pp., 2008.
694 García-Estringana, P., Latron, J., Llorens, P., and Gallart, F.: Spatial and temporal dynamics of soil
695 moisture in a Mediterranean mountain area (Vallcebre, NE Spain), Ecohydrology, 6, 741–753,
696 10.1002/eco.1295, 2013.
697 García-Ruiz, J. M., and Lana-Renault, N.: Hydrological and erosive consequences of farmland
698 abandonment in Europe, with special reference to the Mediterranean region – A review, Agriculture,
699 Ecosystems and Environment, 140, 317–338, 10.1016/j.agee.2011.01.003, 2011.
700 Gea-Izquierdo, G., Montero, G., and Cañellas, I.: Changes in limiting resources determine spatio-
701 temporal variability in tree–grass interactions, Agroforestry Systems, 76, 375-387, 10.1007/s10457-
702 009-9211-4, 2009.
703 Gindel, I.: Seasonal fluctuations in soil moisture under the canopy of xerophytes and in open areas,
704 Commonwealth Forestry Review, 43, 219-234, 19640601878, 1964.
705 Gómez-Gutiérrez, Á., Schnabel, S., and Lavado-Contador, J. F.: Gully erosion, land use and
706 topographical thresholds during the last 60 years in a small rangeland catchment in SW Spain, Land
707 Degradation & Development, 20, 535-550, 10.1002/ldr.931, 2009.
708 Gómez Gutiérrez, J. M., and Luis Calabuig, E.: Producción de praderas y pastizales, in: El libro de las
709 dehesas salmantinas, edited by: Gómez Gutiérrez, J. M., Junta de Castilla y León, Salamanca, 489-
710 511, 1992.
711 González, F., Schnabel, S., Prieto, P. M., Pulido-Fernández, M., and Gragera-Facundo, J.: Pasture
712 productivity in dehesas and its relationship with rainfall and soil, in: Nuevos retos de la ganadería
713 extensiva: un agente de conservación en peligro de extinción, edited by: Canals Tresserras, R. M., and
714 San-Emérito-Garciandía, L., Sociedad Española para el Estudio de los Pastos, Navarra, 37-43, 2012.
715 Hoff, C., and Rambal, S.: An examination of the interaction between climate, soil and leaf area index
716 in a Quercus ilex ecosystem, Annals of Forest Science, 60, 153–161, 10.1051/forest:2003008, 2003.
717 Houérou, H. N., and Hoste, C. H.: Rangeland production and annual rainfall relations in the
718 Mediterranean Basin and in the African Sahelo-Sudanian Zone., Journal of Range Management,
719 30, 181-189, 1977.
720 Infante, J. M., Domingo, F., Fernández-Alés, R., Joffre, R., and Rambal, S.: Quercus ilex transpiration
721 as affected by a prolonged drought period, Biología Plantarum, 46, 49-55,
722 10.1023/A:1022353915578, 2003.
723 Istanbulluoglu, E., Wang, T., and Wedin, D. A.: Evaluation of ecohydrologic model parsimony at local
724 and regional scales in a semiarid grassland ecosystem, Ecohydrology, 5, 121-142, 10.1002/eco.211,
725 2012.
726 Ivanov, V. Y., Bras, R. L., and Curtis, D. C.: A weather generator for hydrological, ecological, and
727 agricultural applications, Water Resources Research, 43, WR005364, 10.1029/2006WR005364, 2007.
728 Ivanov, V. Y., Bras, R. L., and Vivoni, E. R.: Vegetation-hydrology dynamics in complex terrain of
729 semiarid areas: 1. A mechanistic approach to modeling dynamic feedbacks, Water Resources
730 Research, 44, W03429, 10.1029/2006WR005588, 2008.
731 Jarvis, P. G.: The Interpretation of the Variations in Leaf Water Potential and Stomatal Conductance
732 Found in Canopies in the Field, Philosophical Transactions of the Royal Society of London. Series B,
733 Biological Sciences, 273, 593-610, 1976.

734 Jencso, K. G., McGlynn, B. L., Gooseff, M. N., Wondzell, S. M., Bencala, K. E., and Marshall, L. A.:
735 Hydrologic connectivity between landscapes and streams: Transferring reach and plot scale
736 understanding to the catchment scale, Water Resources Research, 45, W04428,
737 10.1029/2008WR007225, 2009.
738 Joffre, R., and Rambal, S.: Soil water improvement by trees in the rangelands of southern Spain,
739 Oecologia Plantarum, 9, 405-422, 1988.
740 Joffre, R., Vacher, J., De los Llanos, C., and Long, G.: The dehesa: an agrosilvopastoral system of the
741 mediterranean region with special reference to the Sierra Morena area of Spain, Agroforestry
742 Systems, 6, 71-96, 10.1007/BF02220110, 1988.
743 Joffre, R., and Rambal, S.: How tree cover influences the water balance of mediterranean rangelands,
744 Ecology, 74, 570-582, 1993.
745 Landsberg, J. J., and Waring, R. H.: A generalised model of forest productivity using simplified
746 concepts of radiation-use efficiency, carbon balance and partitioning, Forest Ecology and
747 Management, 95, 209-228, 10.1016/S0378-1127(97)00026-1, 1997.
748 Lavado-Contador, J. F., Schnabel, S., and Trenado-Ordóñez, R.: Comparison of recent land use and
749 land cover changes in two Dehesa agrosilvopastoral landuse systems, SW Spain, in: Agrosilvopastoral
750 Systems. Dehesas and Montados. Advances in Geoecology, 37, edited by: Schnabel, S., and Ferreira,
751 A., Cáceres, Spain, 55-69, 2004.
752 Lavado-Contador, J. F., Maneta, M., and Schnabel, S.: Prediction of near-surface soil moisture at large
753 scale by Digital Terrain Modeling and Neural Networks, Environmental Monitoring and Assessment,
754 121, 211-230, 10.1007/s10661-005-9116-2, 2006.
755 Lozano-Parra, F. J., Schnabel, S., and Ceballos-Barbancho, A.: Dinámica del agua del suelo en dehesa
756 bajo diferentes cubiertas vegetales. Resultados preliminares, in: Estudios de la Zona No Saturada del
757 Suelo, edited by: Martínez-Fernández, J., and Sanchez Martín, N., Universidad de Salamanca,
758 Salamanca, 47-52, 2011.
759 Maneta, M.: Modelling of the hydrologic processes in a small semiarid catchment, PhD Thesis,
760 Geography and Land Planning Department, University of Extremadura, Cáceres, 278 pp., 2006.
761 Maneta, M., Pasternack, G. B., Wallender, W. W., Jetten, V., and Schnabel, S.: Temporal instability of
762 parameters in an event-based distributed hydrologic model applied to a small semiarid catchment,
763 Journal of Hydrology, 341, 207-221, 10.1016/j.jhydrol.2007.05.010, 2007.
764 Maneta, M., Schnabel, S., and Jetten, V.: Continuous spatially distributed simulation of surface and
765 subsurface hydrological processes in a small semiarid catchment, Hydrological Processes, 22, 2196-
766 2214, 10.1002/hyp.6817, 2008a.
767 Maneta, M., Schnabel, S., Wallender, W. W., Panday, S., and Jetten, V.: Calibration of an
768 evapotranspiration model to simulate soil water dynamics in a semiarid rangeland, Hydrological
769 Processes, 22, 4655-4669, 10.1002/hyp.7087, 2008b.
770 Maneta, M., and Silverman, N.: A spatially-distributed model to simulate water, energy and
771 vegetation dynamics using information from regional climate models, Earth Interactions, 17, 1-44,
772 10.1175/2012EI000472.1, 2013.
773 Martínez Fernández, J., Cano, A., Hernández-Santana, V., and Morán, C.: Evolución de la humedad
774 del suelo bajo diferentes tipos de cubierta vegetal en la cuenca del Duero, Estudios en la Zona No
775 Saturada VIII 257-258, 2007.
776 McGlynn, B. L., McDonnell, J., Stewart, M., and Seibert, J.: On the relationships between catchment
777 scale and streamwater mean residence time, Hydrological Processes, 17, 175-181,
778 10.1002/hyp.5085, 2003.
779 Montaldo, N., Rondena, R., Albertson, J. D., and Mancini, M.: Parsimonious modeling of vegetation
780 dynamics for ecohydrologic studies of water-limited ecosystems, Water Resources Research, 41,
781 W10416, 10.1029/2005WR004094, 2005.
782 Montero, G., San Miguel, A., and Cañellas, I.: System of Mediterranean silviculture “La Dehesa”, in:
783 Agricultura Sostenible, edited by: Jiménez Díaz, R. M., and Lamo de Espinos, J., Mundi Prensa,
784 Madrid, 1998.

785 Montero, M. J., Moreno, G., and Bertomeu, M.: Light distribution in scattered-trees open woodlands
786 in Western Spain, Agroforestry Systems, 73, 233–244, 10.1007/s10457-008-9143-4, 2008.
787 Moreno, G., Obrador, J. J., Cubera, E., and Dupraz, C.: Fine root distribution in Dehesas of Central-
788 Western Spain, Plant and Soil, 277, 153-162, 10.1007/s11104-005-6805-0, 2005.
789 Moreno, G.: Response of understorey forage to multiple tree effects in Iberian dehesas, Agriculture,
790 Ecosystems and Environment, 123, 239-244, 10.1016/j.agee.2007.04.006, 2008.
791 Moreno, G., and Cubera, E.: Impact of stand density on water status and leaf gas exchange in
792 Quercus ilex, Forest Ecology and Management, 254, 74-84, 10.1016/j.foreco.2007.07.029, 2008.
793 Ogaya, R., and Peñuelas, J.: Phenological patterns of Quercus ilex, Phillyrea latifolia, and Arbutus
794 unedo growing under a field experimental drought, Ecoscience, 11, 263-270, 2004.
795 Oleson, K. W., Lawrence, D. M., Bonan, G. B., Flanner, M. G., and Kluzek, E.: Technical Description of
796 version 4.0 of the Community Land Model (CLM), NCAR. Boulder, CO, 10.5065/D6FB50WZ, 2010.
797 Paço, T. A., David, T. S., Henriques, M. O., Pereira, J. S., Valente, F., Banza, J., Pereira, F. L., Pinto, C.,
798 and David, J. S.: Evapotranspiration from a Mediterranean evergreen oak savannah: The role of trees
799 and pasture, Journal of Hydrology, 369, 98-106, 10.1016/j.jhydrol.2009.02.011, 2009.
800 Panaïotis, C., Carcaillet, C., and M'Hamedi, M.: Determination of the natural mortality age of a holm
801 oak (Quercus ilex L.) stand in Corsica (Mediterranean Island) Oecologia, 18, 519-530, 1997.
802 Plaixats, J., Villareal, A., Bartolomé, J., and Espona, J.: Productivity characteristics of grassland in a
803 dehesa system in Catalonia, Spain, in: Sustainability of agrosilvopastoral systems - Dehesas,
804 Montados -. Advances in geoecology, edited by: Schnabel, S., and Ferreira, A., Catena Verlag,
805 Reiskirchen, Germany, 195-202, 2004.
806 Porporato, A., D'Odorico, P., Laio, F., Ridolfi, L., and Rodriguez-Iturbe, I.: Ecohydrology of water-
807 controlled ecosystems, Advances in Water Resources, 25, 1335-1348, Doi: 10.1016/s0309-
808 1708(02)00058-1, 2002.
809 Ricotta, C., Avena, G. C., and Teggi, S.: Relation between vegetation canopy surface temperature and
810 the Sun-surface geometry in a mountainous region of central Italy, Remote Sensing, 18:14, 3091-
811 3096, 1997.
812 Richardson, C. W.: Stochastic simulation of daily precipitation, temperature, and solar radiation,
813 Water Resources Research, 17, 182-190, 10.1029/WR017i001p00182, 1981.
814 Rivest, D., Rolo, V., López-Díaz, L., and Moreno, G.: Shrub encroachment in Mediterranean
815 silvopastoral systems: Retama sphaerocarpa and Cistus ladanifer induce contrasting effects on
816 pasture and Quercus ilex production, Agriculture, Ecosystems and Environment, 141, 447-454,
817 10.1016/j.agee.2011.04.018, 2011.
818 Rodriguez-Iturbe, I., D'Odorico, P., Porporato, A., and Ridolfi, L.: On the Spatial and Temporal Links
819 Between Vegetation, Climate, and Soil Moisture, Water Resour. Res., 35, 10.1029/1999wr900255,
820 1999.
821 Rodríguez-Iturbe, I.: Ecohydrology: A hydrologic perspective of climate-soil-vegetation dynamics,
822 Water Resources Research, 36, 3-9, 10.1029/1999WR900210, 2000.
823 Sabaté, S., Gracia, C., and Sánchez, A.: Likely effects of climate change on growth of Quercus ilex,
824 Pinus halepensis, Pinus pinaster, Pinus sylvestris and Fagus sylvatica forests in the Mediterranean
825 region, Forest Ecology and Management, 5906, 1-15, 10.1016/S0378-1127(02)00048-8, 2002.
826 Santamaría, O., Poblaciones, M. J., Olea, L., Rodrigo, S., and García-White, T.: Efecto de fertilizantes
827 alternativos al superfosfato de cal sobre la producción y calidad de pastos de dehesa en el suroeste
828 de España, 5º Congreso Forestal Español, Ávila, 2009.
829 Schnabel, S.: Soil erosion and runoof production in small watershed under silvo-pastoral landuse
830 (dehesas) in Extremadura, Spain, Monografías Científicas. Geoforma, Logroño, 163 pp., 1997.
831 Schnabel, S.: La precipitación como factor en los procesos hidrológicos y erosivos. Análisis de datos
832 de Cáceres capital., in: Hidrología y erosión de suelos., edited by: Schnabel, S., Gómez-Amelia, D., and
833 Ceballos-Barbancho, A., Norba. Revista de Geografía., Cáceres, 137-152, 1998.
834 Schnabel, S., Dahlgren, R. A., and Moreno, G.: Soil and water dynamics, in: Mediterranean oak
835 woodland working landscapes. Dehesas of Spain and rangelands of California, edited by: Campos, P.,

836 Huntsinger, L., Oviedo, J. L., Starrs, P. F., Díaz, M., Standiford, R., and Montero, G., Springer-Verlag,
837 New York, 2013a.
838 Schnabel, S., Pulido Fernández, M., and Lavado-Contador, J. F.: Soil water repellency in rangelands of
839 Extremadura (Spain) and its relationship with land management, Catena, 103, 53-61,
840 10.1016/j.catena.2011.11.006, 2013b.
841 Semenov, M. A., and Porter, J. R.: Climatic variability and the modelling of crop yields, Agricultural
842 and Forest Meteorology, 73, 265-283, 10.1016/0168-1923(94)05078-K, 1995.
843 Semenov, M. A., and Barrow, E. M.: Use of a stochastic weather generator in the development of
844 climate change scenarios, Climate Change, 35, 397-414, 10.1023/A:1005342632279, 1997.
845 Semenov, M. A., Brooks, R. J., Barrow, E. M., and Richardson, C. W.: Comparison of the WGEN and
846 LARS-WG stochastic weather generators for diverse climates, Climate Research, 10, 95-107, 1998.
847 Semenov, M. A., and Barrow, E. M.: LARS-WG: A Stochastic Weather Generator for Use in Climate
848 Impact Studies, User Manual http://www.rothamsted.ac.uk/mas-models/larswg.php, 2002.
849 Singh, V. P.: Kinematic wave modeling in water resources. Environmental hydrology, Wiley
850 Interscience, New York, 830 pp., 1997.
851 Swinbank, W. C.: Long-wave radiation from clear skies, Quarterly Journal of the Royal Meteorological
852 Society, 90, 488-493, 10.1002/qj.49708938105, 1964.
853 Tague, C. L., and Band, L. E.: RHESSys: Regional Hydro-Ecologic Simulation System-An Object-
854 Oriented Approach to Spatially Distributed Modeling of Carbon, Water, and Nutrient Cycling, Earth
855 Interactions, 8, 2004.
856 Tubiello, F. N., Soussana, J. F., and Howden, S. M.: Crop and pasture response to climate change,
857 PNAS, 104, 19686-19690, 10.1073/pnas.0701728104 2007.
858 Van Schaik, L., Schnabel, S., and Jetten, V.: The influence of preferencial flow on hillslope hydrology in
859 a semi-arid watershed (in the Spanish Dehesas), Hydrological Processes, 22, 3844-3855,
860 10.1002/hyp.6998, 2008.
861 Van Schaik, L.: Spatial variability of infiltration patterns related to site characteristics in a semi-arid
862 watershed, Catena, 78, 36-47, 10.1016/j.catena.2009.02.017, 2009.
863 Van Schaik, L.: The role of macropore flow from plot a catchment scale, Faculteit
864 Geowetenschappen, Universiteit Utrecht, Utrecht, 174 pp., 2010.
865 Vaz, M., Maroco, J., Ribeiro, N., Gazarini, L. C., Pereira, J. S., and Chaves, M. M.: Leaf-level responses
866 to light in two co-occurring Quercus (Quercus ilex and Quercus suber): leaf structure, chemical
867 composition and photosynthesis, Agroforestry Systems, 82, 173-181, 10.1007/s10457-010-9343-6,
868 2011.
869 Viville, D., and Littlewood, I. G.: Ecohydrological processes in small basins, edited by: Viville, D., and
870 Littlewood, I. G., UNESCO, Strasbourg (France), 199 pp., 1996.
871 Wang, L., Liu, J., Sun, G., Wei, X., Liu, S., and Dong, Q.: Water, climate, and vegetation: ecohydrology
872 in a changing world, Hydrology and Earth System Sciences, 16, 4633-4636, 10.5194/hess-16-4633-
873 2012, 2012.
874 White, M. A., Thornton, P. E., Running, S. W., and Nemani, R. R.: Parameterization and Sensitivity
875 Analysis of the BIOME–BGC Terrestrial Ecosystem Model: Net Primary Production Controls, Earth
876 Interact., 4, 1–85, 10.1175/1087-3562(2000)004<0003:PASAOT>2.0.CO;2, 2000.
877 Xia, J.: A stochastic weather generator applied to hydrological models in climate impact analysis,
878 Theoretical and Applied Climatology, 55, 177-183, 10.1007/BF00864713, 1996.

879

880

881 Table 1. List of vegetation parameters used in this study. Variable symbols match those in Maneta and

882 Silverman (2013)

| Variable | Description | Unit | Value | | Source |
|---|---|---|---|---|---|
| | | | Tree | Pasture | |
| $\xi_c$ | Canopy quantum efficiency | gC $J^{-1}$ | 1.8 E-06 | 1.8 E-06 | Landsberg and Waring (1997) and Vaz et al. (2011) |
| $F_{\mathrm{pra}}$ | Carbon allocation parameter | – | 2.235 | - | Landsberg and Waring (1997) |
| $F_{\mathrm{prn}}$ | Carbon allocation parameter | – | 0.006 | - | Landsberg and Waring (1997) |
| $S_{\mathrm{pra}}$ | Carbon allocation parameter | – | 3.3 | - | Landsberg and Waring (1997) |
| $S_{\mathrm{prn}}$ | Carbon allocation parameter | – | 9.00E-07 | - | Landsberg and Waring (1997) |
| $\Phi_{s\downarrow}$ | Empirical coefficient of the solar radiation efficiency function for canopy resistance | – | 350 | 350 | Cox et al. (1998) |
| $\Phi_{ea}$ | Empirical coefficient of the vapor pressure efficiency function for canopy resistance | – | 0.0019 | 0.0019 | Cox et al. (1998) |
| $\Phi_{\theta}$ | Empirical coefficient of the soil moisture efficiency function for canopy resistance | – | 2 | 2 | Cox et al. (1998) |
| $\omega$ | Crown to stem diameter ratio | – | 0.57 | - | |
| $\rho_{\mathrm{wood}}$ | Density of wood | gC $m^{-3}$ | 930000 | - | Barboutis and Philippou (2007) |
| $F_{hd\mathrm{max}}$ | Maximum allowed height to stem diameter | – | 22.2 | - | Infante et al. (2003) |
| $F_{hd\mathrm{min}}$ | Minimum allowed height to stem diameter | – | 6.6 | - | |
| $\delta_{\mathrm{r}}$ | Root Turnover Rate | $s^{-1}$ | 2.85E-08 | 2.85E-08 | Only for fine roots, from Hoff and Rambal (2003) |
| $\alpha$ | Albedo of canopies | - | 0.12 | 0.2 | Cox et al. (1999) |
| $\varepsilon_c$ | Emissivity and absorptivity of canopies | - | 0.97 | 0.97 | Ricotta et al. (1997) |
| $k$ | Beer´s law exponential attenuation coefficient | – | 0.4 | 0.4 | White et al. (2000) |
| age | Effective age of tree stand | yr | 170 | - | Panaïotis et al. (1997) |
| $H_t$ | Effective tree height | m | 7.6 | - | Infante et al. (2003) |

883

884

885

886 Table 2. Set of model parameters included in the process of manual calibration. *Values vary spatially.

| Variable | Description | Unit | Final value | | Source for initial values |
|---|---|---|---|---|---|
| | | | Tree | Pasture | |
| $C_{NPP}$ | GPP to NPP conversion factor | – | 0.25 | 0.35 | Sabaté et al. (2002) |
| $T_{opt}$ | Optimal Temperature for maximum plant growth | ºC | 15 | 18 | Ogaya and Peñuelas (2004); and AEMET |
| $T_{max}$ | Maximum Temperature for plant | ºC | 42.6 | 30 | AEMET |
| $T_{min}$ | Minimum Temperature for plant | ºC | -5.6 | 2 | AEMET |
| $k_{sd}$ | Dry grass turnover rate | – | - | 8.50E-07 | adjusted |
| $T_{\xi}$ | Temperature for enhanced grass decay | ºC | - | 18 | adjusted |
| $\delta_f$ | Leaf Turnover Rate | $s^{-1}$ | 1.40E-08 | 1.00E-07 | Hoff and Rambal (2003) |
| $\sigma_{LAI}$ | Specific Leaf Area | $m^2\,gC^{-1}$ | 0.017 | 0.015 | Vaz et al. (2011) |
| $\xi_w$ | Vegetation water use efficiency | $gC\ m^{-1}$ | 1150 | 6000 | Hoff and Rambal (2003) |
| $X_{stor\ max}$ | Maximum canopy water storage per unit LAI | m | 0.00075 | 0.00015 | White et al. (2000) |
| $g_{cmax}$ | Maximum stomatal conductance | $m\ s^{-1}$ | 0.0063 | 0.035 | White et al. (2000) |
| $\theta_{wp}$ | Volumetric soil moisture content at wilting point | $m^3\,m^{-3}$ | 0.05 | 0.165 | Van Schaik (2010) |
| $K_{eff}$ * | Effective hydraulic conductivity of the soil | $m\ s^{-1}$ | 0.00479 – 0.00053 | | measured |
| $\eta$ * | Soil Porosity | 0 – 1 | 0.50 – 0.26 | | measured |
| $\lambda$ * | Brooks and Corey exponent parameter | – | 0.33 – 0-20 | | adjusted |

887

888

889

890 Table 3. Goodness-of-fit between observed and simulated weather data. *K-S* = Kolmogorov–Smirnov
891 test; * = Example data: *Obs*. = Observed average values from the study catchment (2000-2012); *Sim*. =
892 Simulated average values for 300 years.

| | *** Rainfall** | | **Rainfall** | | **Maximum Temperature** | | **Minimum Temperature** | | **Short Wave Radiation** | |
|---|---|---|---|---|---|---|---|---|---|---|
| | *Obs.* | *Sim.* | *K-S* | *p-value* | *K-S* | *p-value* | *K-S* | *p-value* | *K-S* | *p-value* |
| **Jan.** | 45.0 | 44.4 | 0.033 | 1.000 | 0.053 | 1.000 | 0.106 | 0.999 | 0.044 | 1.000 |
| **Feb.** | 52.5 | 60.7 | 0.042 | 1.000 | 0.106 | 0.999 | 0.106 | 0.999 | 0.087 | 1.000 |
| **Mar.** | 43.1 | 45.1 | 0.035 | 1.000 | 0.053 | 1.000 | 0.053 | 1.000 | 0.000 | 1.000 |
| **April** | 44.2 | 45.8 | 0.061 | 1.000 | 0.106 | 0.999 | 0.106 | 0.999 | 0.087 | 1.000 |
| **May** | 39.3 | 47.3 | 0.054 | 1.000 | 0.053 | 1.000 | 0.106 | 0.999 | 0.087 | 1.000 |
| **June** | 12.7 | 11.7 | 0.063 | 1.000 | 0.106 | 0.999 | 0.106 | 0.999 | 0.131 | 0.982 |
| **July** | 0.5 | 0.7 | 0.497 | 0.004 | 0.106 | 0.999 | 0.106 | 0.999 | 0.087 | 1.000 |
| **Aug.** | 6.5 | 8.4 | 0.209 | 0.643 | 0.106 | 0.999 | 0.106 | 0.999 | 0.131 | 0.982 |
| **Sept.** | 25.1 | 24.4 | 0.154 | 0.927 | 0.053 | 1.000 | 0.053 | 1.000 | 0.044 | 1.000 |
| **Oct.** | 95.5 | 82.5 | 0.098 | 1.000 | 0.105 | 0.999 | 0.106 | 0.999 | 0.044 | 1.000 |
| **Nov.** | 61.2 | 72.8 | 0.030 | 1.000 | 0.053 | 1.000 | 0.105 | 0.999 | 0.043 | 1.000 |
| **Dec.** | 62.2 | 64.8 | 0.040 | 1.000 | 0.106 | 0.999 | 0.053 | 1.000 | 0.044 | 1.000 |

893

Table 4. Descriptive statistics of observed (Obs.) and simulated (Sim.) series and quality parameters of the model. *n* = sample size; RMSE = Root Mean Square Error; * Values only showed for 2011 because it is the more monitored year.

| | ***n*** | **Average** | | **Maximum** | | **Minimum** | | **Standard Deviation** | | $r^2$ | **RMSE** | **Bias** | **Nash-Sutcliffe** |
|---|---|---|---|---|---|---|---|---|---|---|---|---|---|
| | | *Obs.* | *Sim.* | *Obs.* | *Sim.* | *Obs.* | *Sim.* | *Obs.* | *Sim.* | | | | |
| **Soil Moist.** ($m^3 m^{-3}$) | | | | | | | | | | | | | |
| *Site 1* | 1268 | .219 | .202 | .417 | .430 | .060 | .075 | .108 | .091 | 0.85 | .047 | .018 | 0.81 |
| *Site 2* | 1267 | .222 | .212 | .451 | .440 | .074 | .083 | .114 | .094 | 0.90 | .040 | .010 | 0.88 |
| *SMS-3* | 848 | .165 | .151 | .312 | .349 | .066 | .068 | .069 | .061 | 0.80 | .034 | .014 | 0.75 |
| **Soil Temp.** (°C) | | | | | | | | | | | | | |
| *Site 1* | 1274 | 18.0 | 19.8 | 37.0 | 47.1 | -2.0 | 2.5 | 10.2 | 10.0 | 0.89 | 3.78 | -1.8 | 0.86 |
| *Site 2* | 1267 | 18.1 | 19.0 | 33.4 | 42.7 | 3.2 | 1.9 | 8.2 | 9.5 | 0.91 | 3.08 | -0.9 | 0.86 |
| **Pasture Production** (kg DM $ha^{-1}$) | | | | | | | | | | | | | |
| *Site 1* | 20* | 603.3 | 588.1 | 1319.3 | 1368.7 | 269.0 | 319.0 | 396.2 | 310.2 | 0.84 | 164.8 | 15.2 | 0.82 |
| *Site 2* | 20* | 644.3 | 673.6 | 1392.7 | 1432.5 | 293.4 | 361.5 | 395.3 | 317.4 | 0.76 | 193.4 | -29.3 | 0.75 |

Table 5. Descriptive statistics for simulated rainfall (*mm*) and simulated average pasture production (*kg DM* $ha^{-1}year^{-1}$) for each site and 300 years.

| | ***n*** | **Mean** | **Maximum** | **Minimum** | **Percentile** | | | **SD** |
|---|---|---|---|---|---|---|---|---|
| | | | | | **25** | **50** | **75** | |
| ***Rainfall*** | 300 | 508.7 | 934.1 | 188.9 | 426.7 | 503.7 | 571.9 | 118.2 |
| ***Site 1*** | 300 | 338.0 | 977.6 | 20.7 | 210.0 | 305.9 | 445.1 | 172.5 |
| ***Site 2*** | 300 | 456.0 | 1030.9 | 29.9 | 319.9 | 435.4 | 570.6 | 182.8 |

Table 6. Annual pasture production at *Site 1* and *Site 2* (*kg DM ha$^{-1}$*), annual rainfall (*mm*) and accumulated antecedent rainfall prior to June 1$^{st}$ (30, 60, 90, 120 days).

| **Year** | **207** | **208** | **209** | **210** | **211** | **212** | **213** | **214** | **215** | **216** |
|---|---|---|---|---|---|---|---|---|---|---|
| Production *Site 1* | 78.5 | 288.7 | 361.2 | 446.0 | 594.5 | 745.2 | 592.3 | 503.1 | 120.6 | 339.2 |
| Production *Site 2* | 369.1 | 434.5 | 452.2 | 639.8 | 691.6 | 787.4 | 786.0 | 672.3 | 305.7 | 508.7 |
| Annual rainfall | 276.2 | 476.1 | 549.6 | 534.8 | 519.8 | 866.1 | 531.4 | 361.3 | 309.3 | 373.8 |
| Antecedent rainfall 30 days | 26.4 | 59.3 | 51.3 | 56.8 | 94.9 | 99.1 | 22.8 | 25.3 | 11.5 | 52.2 |
| Antecedent rainfall 60 days | 51.6 | 79.4 | 95.7 | 58.6 | 153.1 | 164.7 | 50.2 | 46.7 | 60.7 | 81.6 |
| Antecedent rainfall 90 days | 73.2 | 131.7 | 168.0 | 108.5 | 155.6 | 194.5 | 83.3 | 96.8 | 79.2 | 112.4 |
| Antecedent rainfall 120 days | 73.2 | 160.9 | 231.1 | 123.3 | 263.1 | 388.0 | 235.0 | 152.7 | 79.2 | 112.4 |

Figure 1. Location of the study catchment and the equipment.

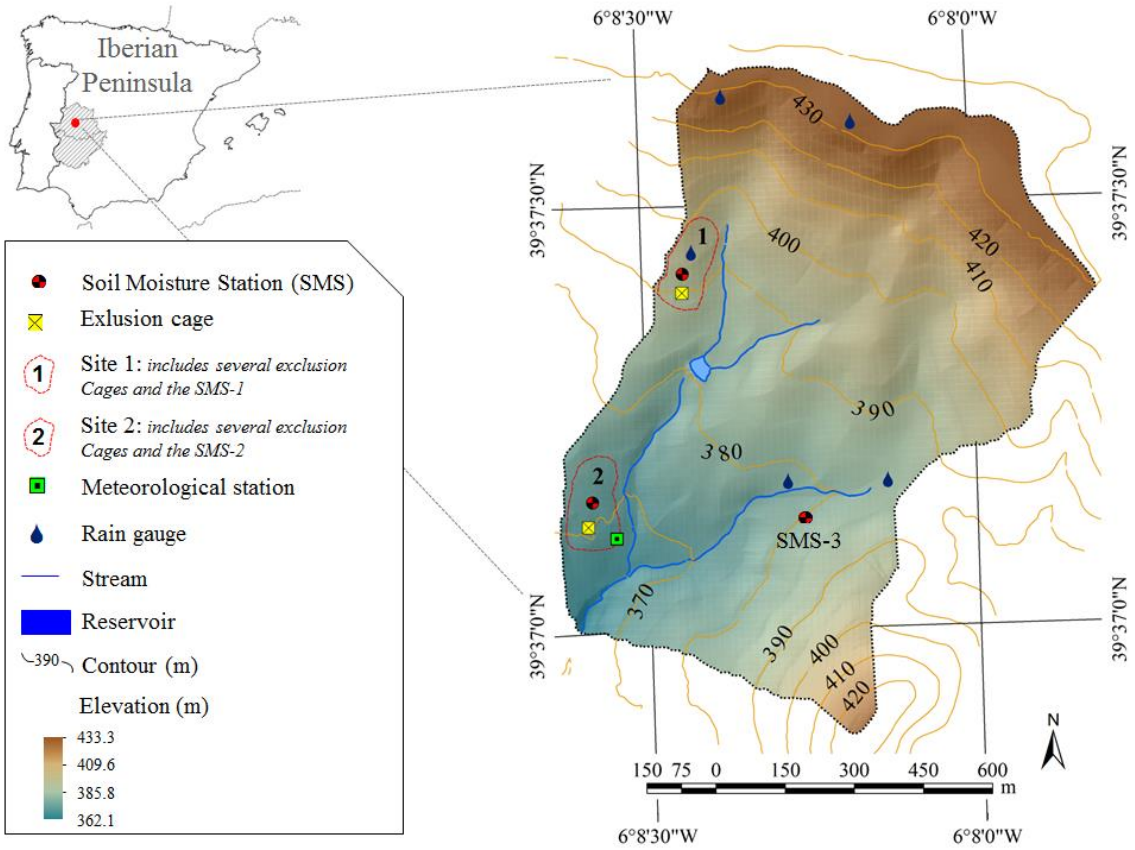

Figure 2. Maps of catchment properties: A) slope (*m/m*), B) soil depth (*m*), C) porosity (0–1), D) flux accumulation (number of pixels that spill on another), E) tree density (*trees* $ha^{-1}$), F) tree canopy cover (0–1). Maps were obtained as described in Maneta et al. (2008).

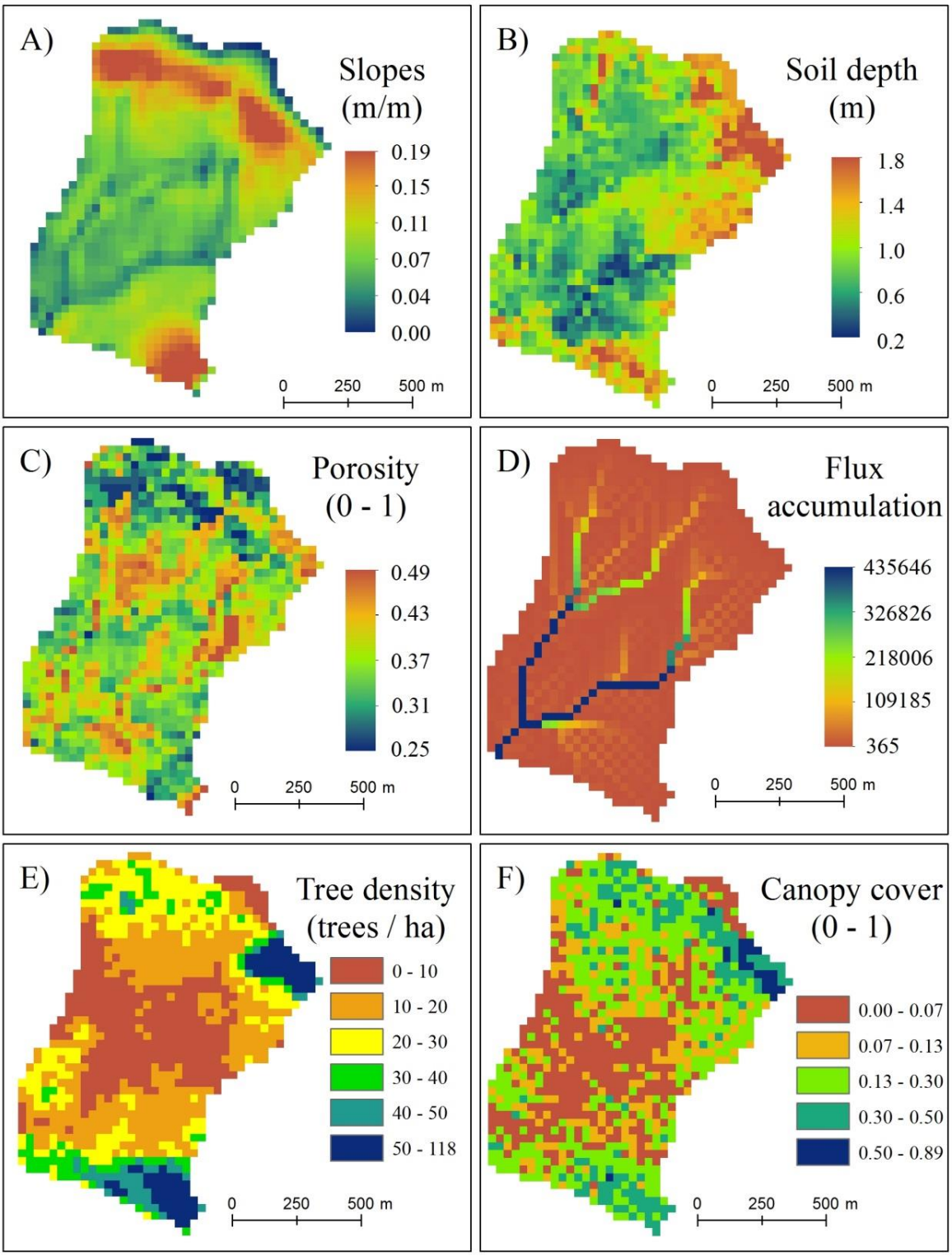

Figure 3: Observed and simulated soil moisture from March 2009 until September 2012. A) Site-1; B) Site-2; C) SMS-3. *Black line* are measured values, and *red line* are simulated values.

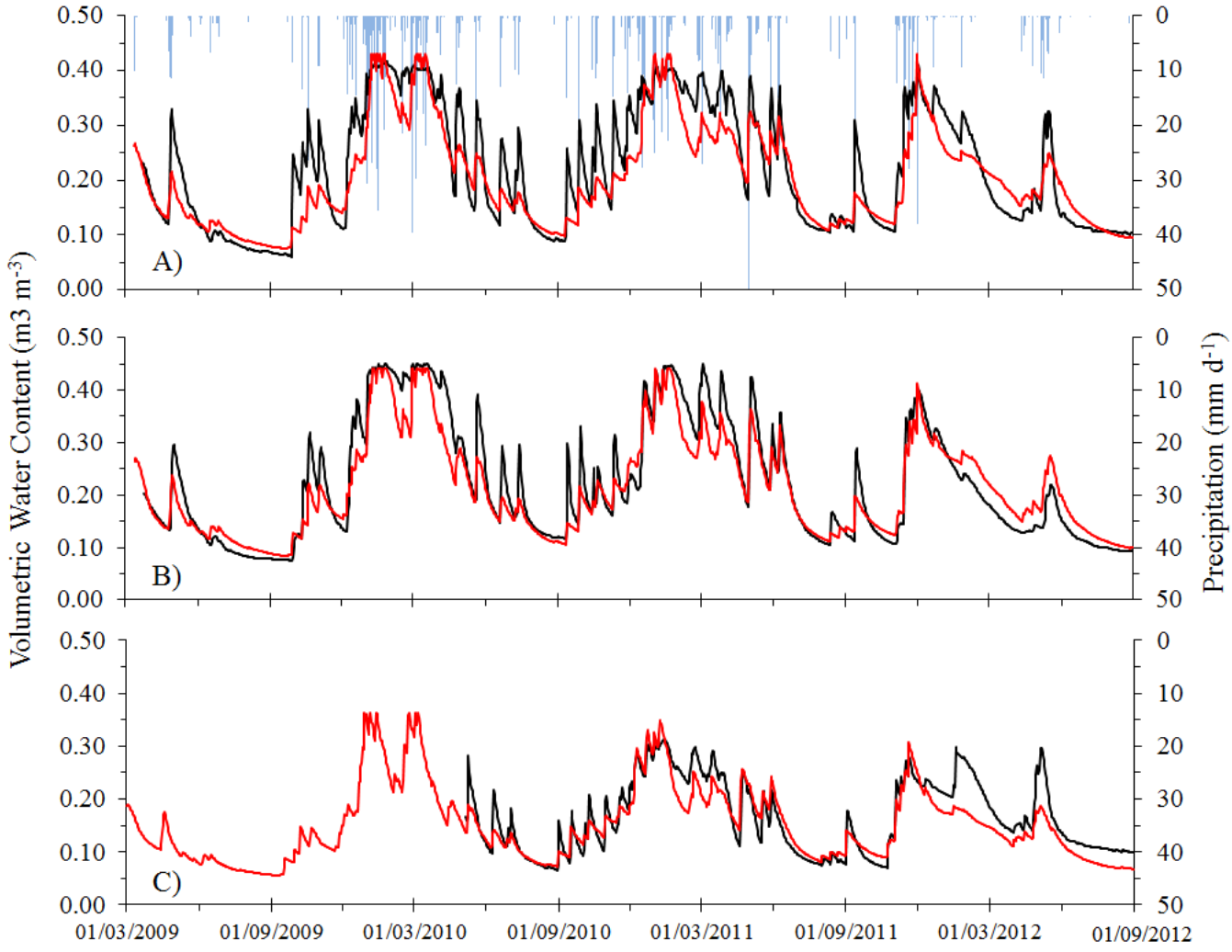

Figure 4: Observed and simulated soil temperature from March 2009 until September 2012. A) Site-1; B) Site-2; *Black line* are measured values, and *red line* are simulated values.

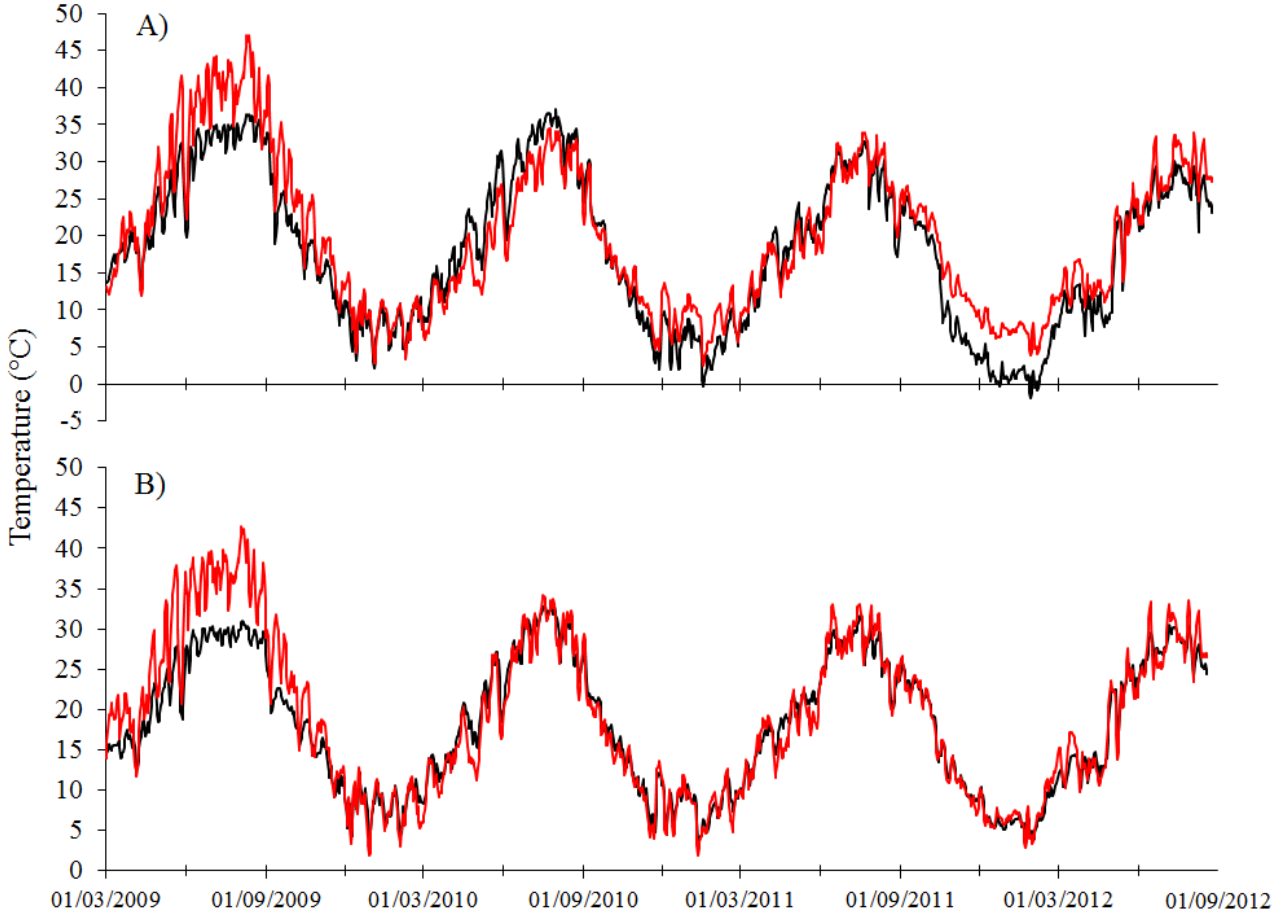

Figure 5: Observed and simulated accumulated pasture production at A) *Site 1*; and B) *Site 2*. The red line represents simulated average pasture yield for whole pixels in every Site, with +/- 1 standard deviation (green shade). Green circles represent average pasture production based on height measurements; blue rhombuses represent average pasture production based on plant cuts (moustaches correspond to +/- standard deviation).

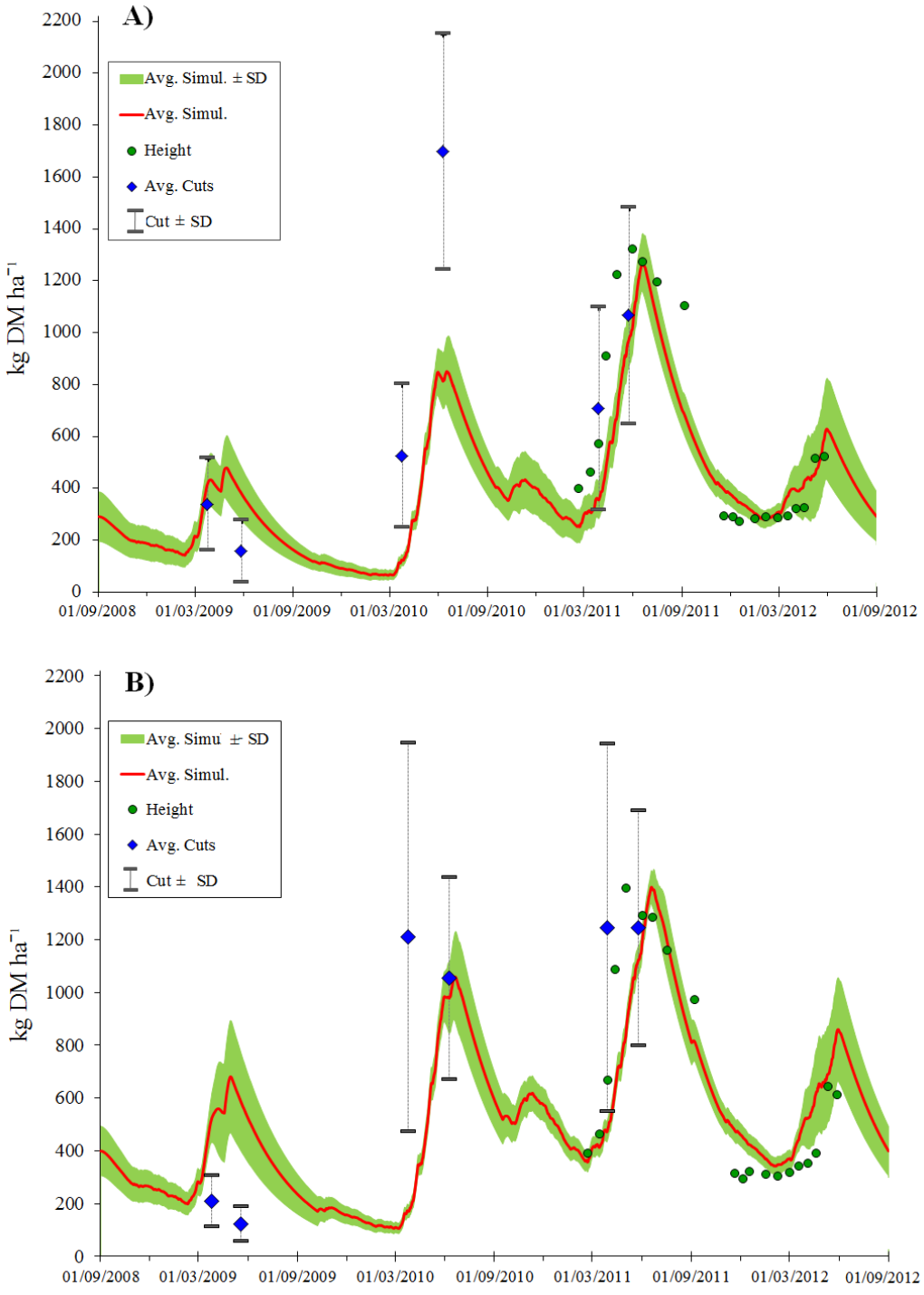

Figure 6. Simulated transpiration during 4 hydrological years (2008-2012) for A) *Quercus ilex* in *Site 1*, and B) natural pastures in *Site 1* and *Site 2*.

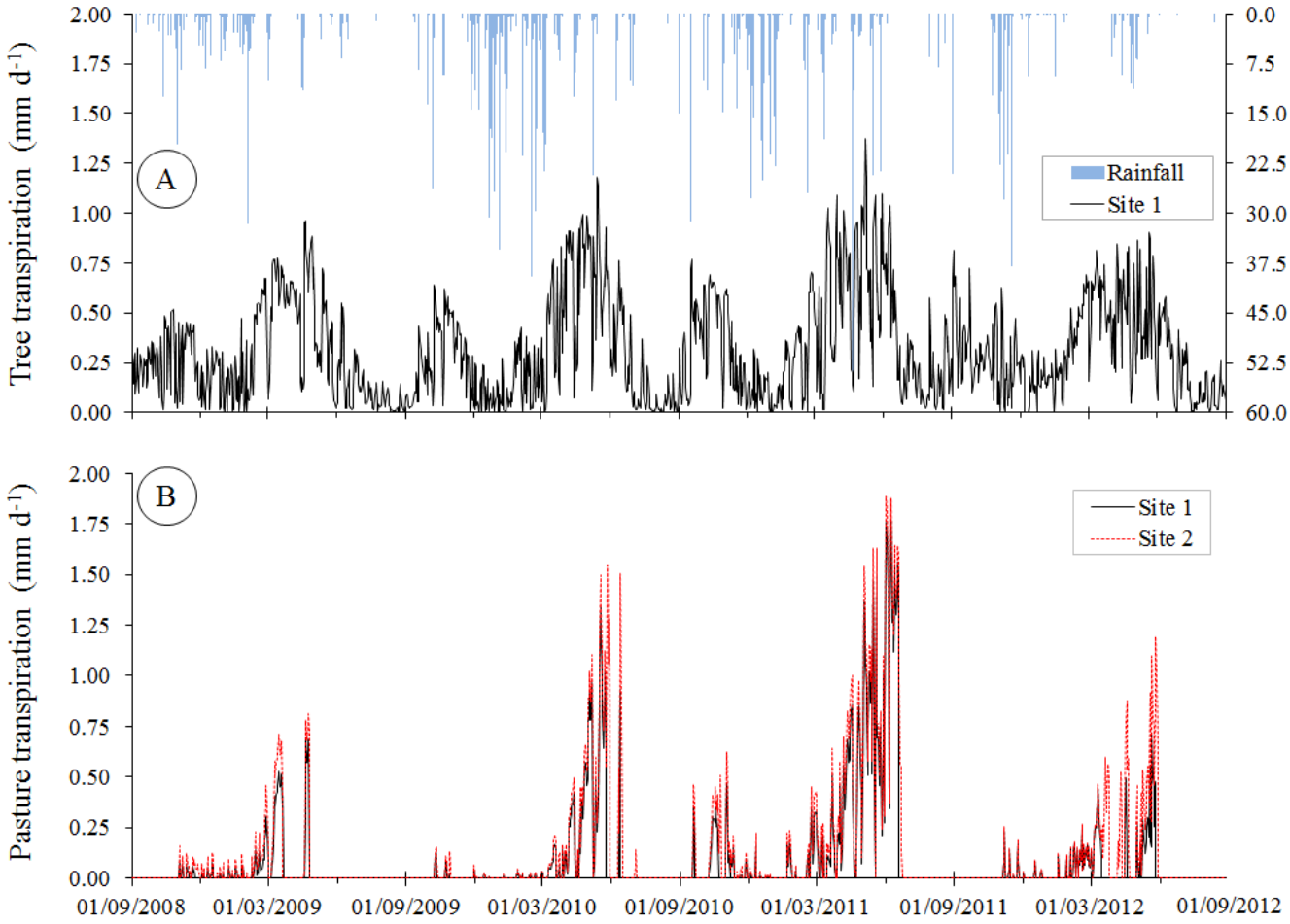

Figure 7. Spatial distribution of annual average soil moisture ($m^3$ $m^{-3}$) (A) and its standard deviation (B), and annual average evapotranspiration (C) (mm).

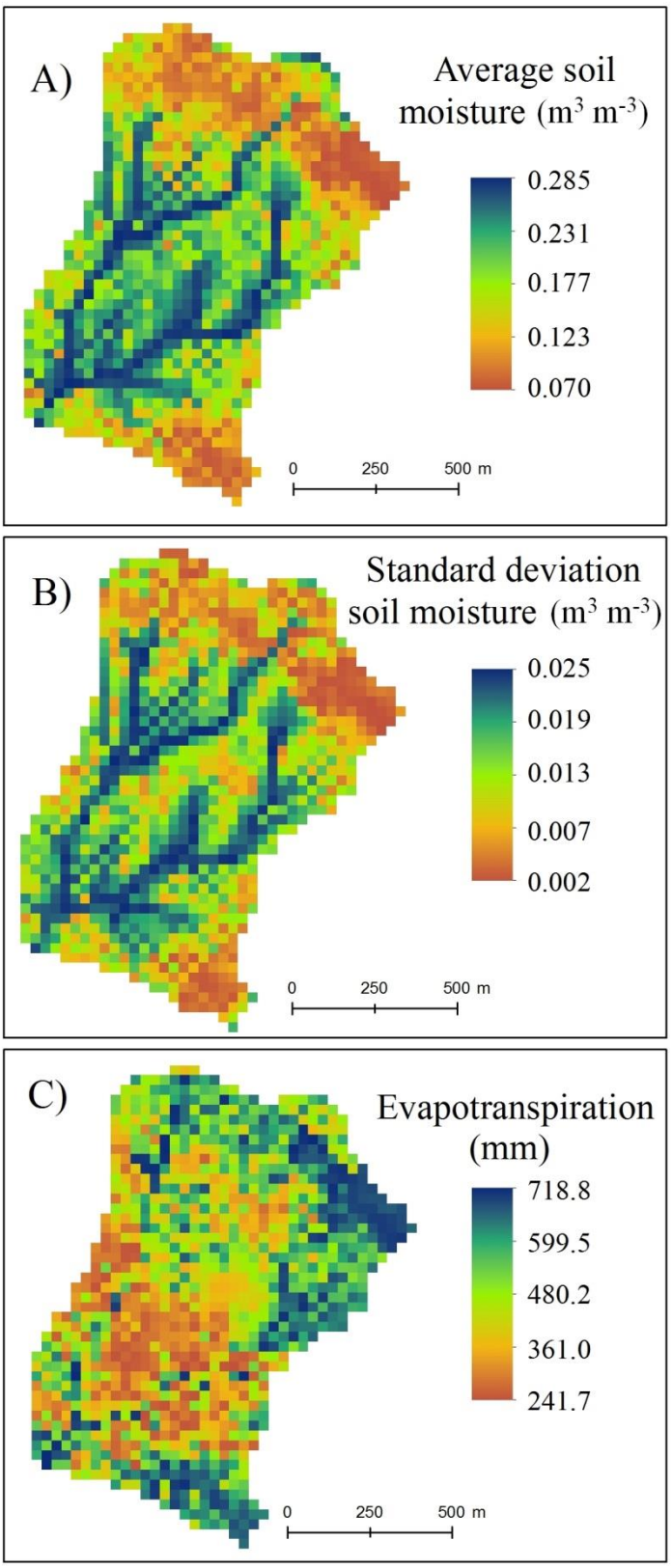

Figure 8. Simulated average pasture production and precipitation at *Site 1*, A) at the annual timescale for 300 years. B) for ten years at the daily timescale (the green shade represents +/- 1 standard deviation of pasture production, and the blue bars is the rainfall)

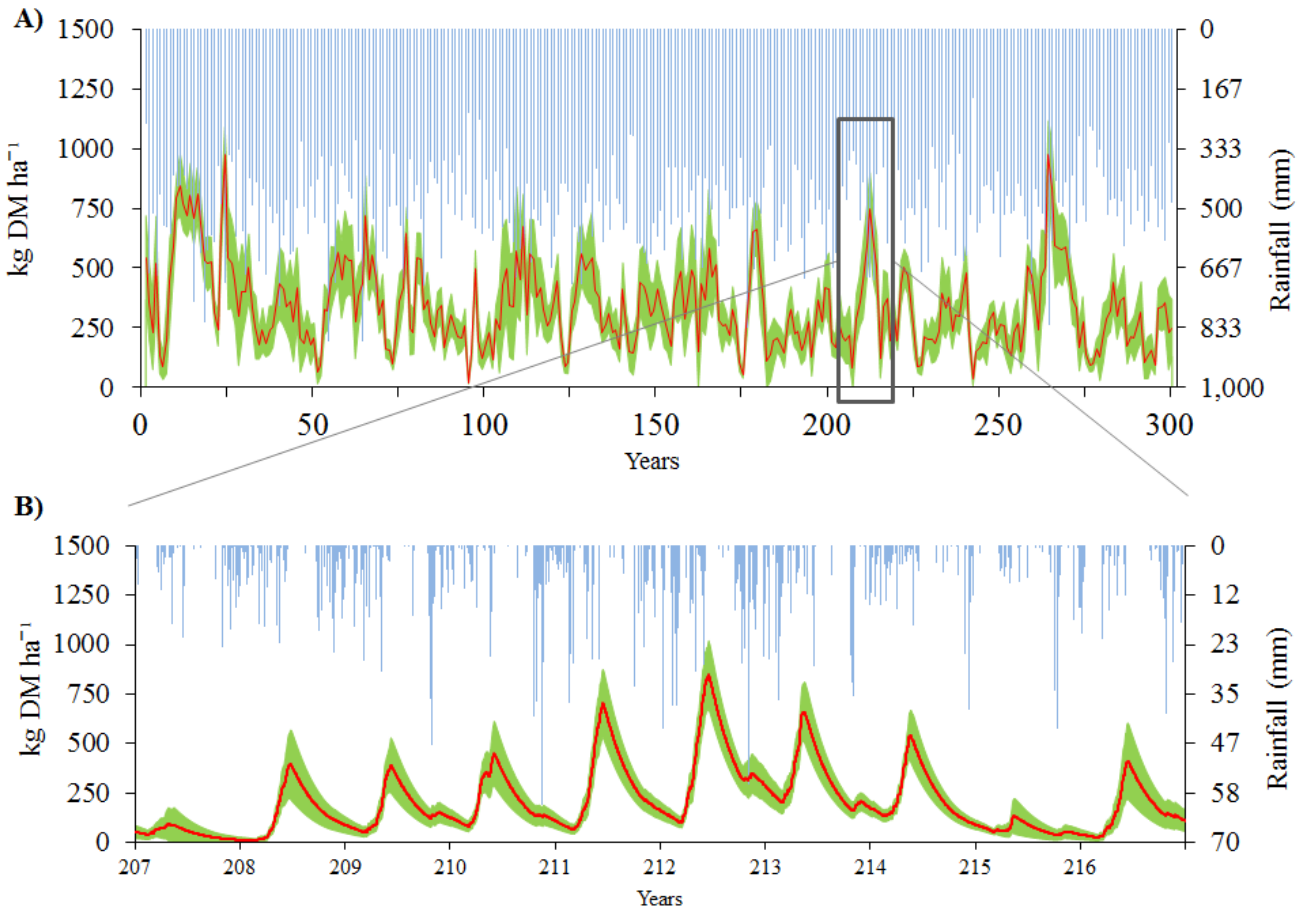

Figure 9. Simulated average pasture production and precipitation at *Site 2*, A) at the annual timescale for 300 years. B) for ten years at the daily timescale (the green shade represents +/- 1 standard deviation of pasture production, and the blue bars is the rainfall)

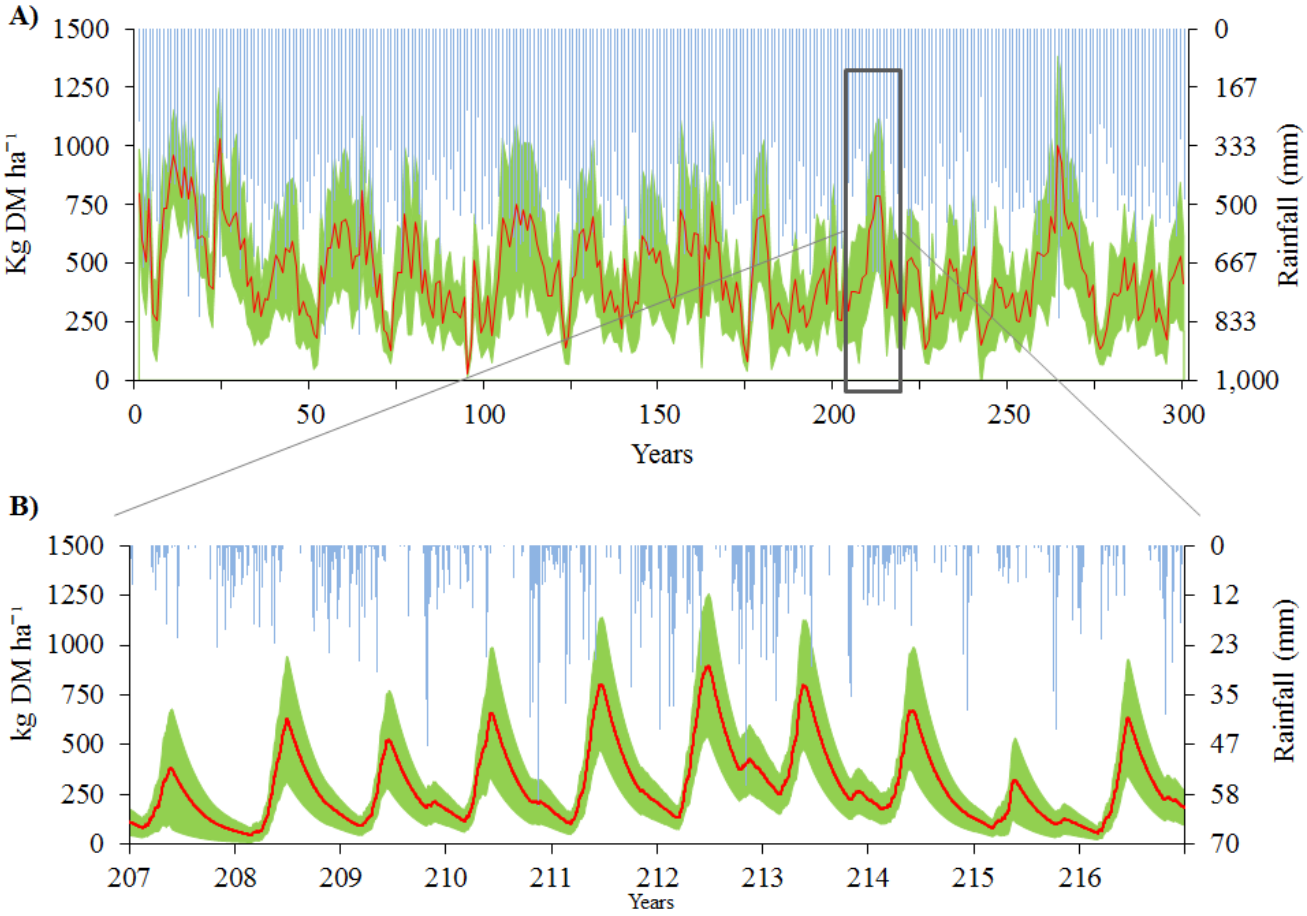

Figure 10. Spatial distribution of simulated pasture production (*kg DM ha$^{-1}$*): A) Average; B) Standard deviation; C) Maximum; D) Minimum.

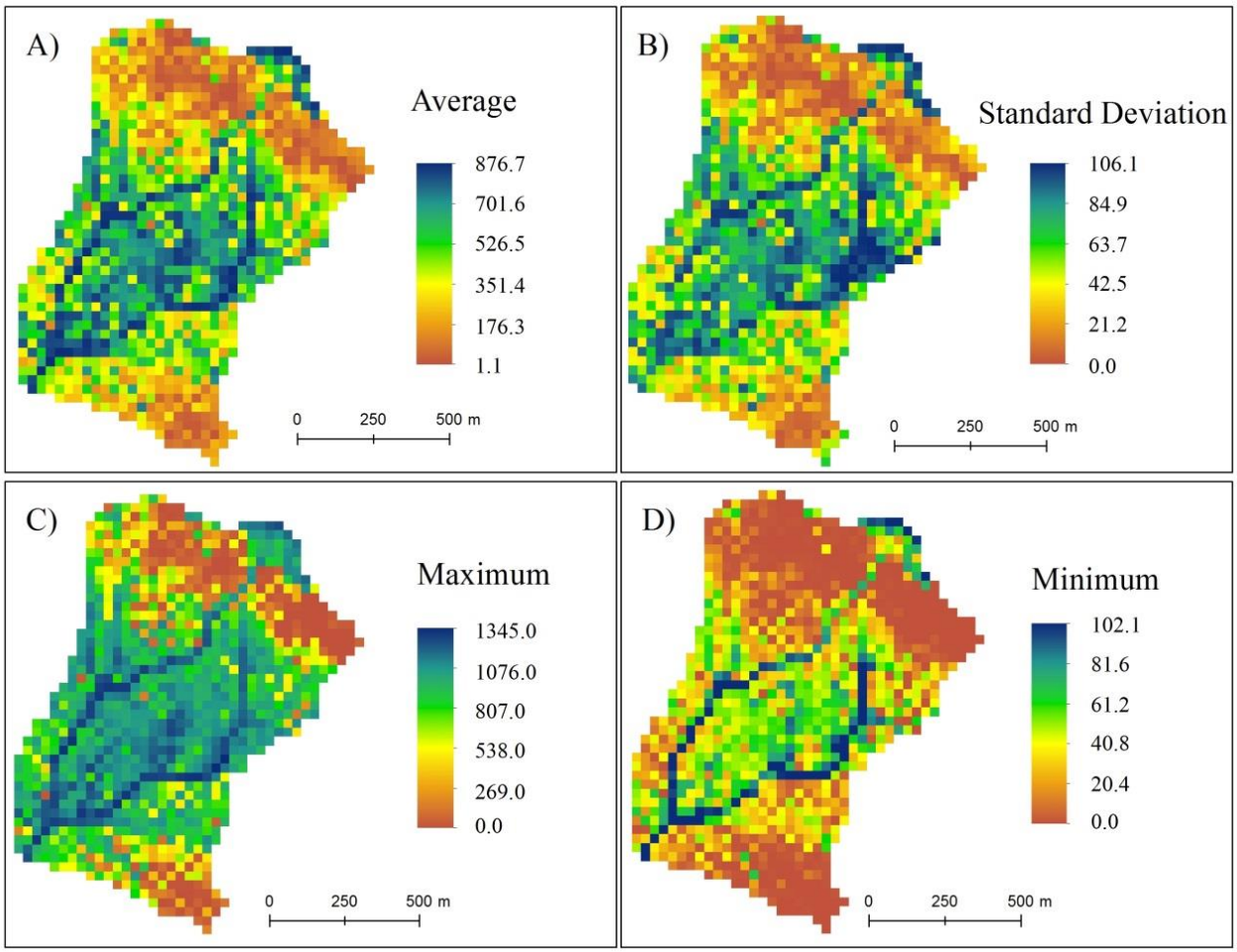

Figure 11. Scatterplot between average pasture production simulated and A) average soil moisture simulated, B) slope, and C) canopy cover.

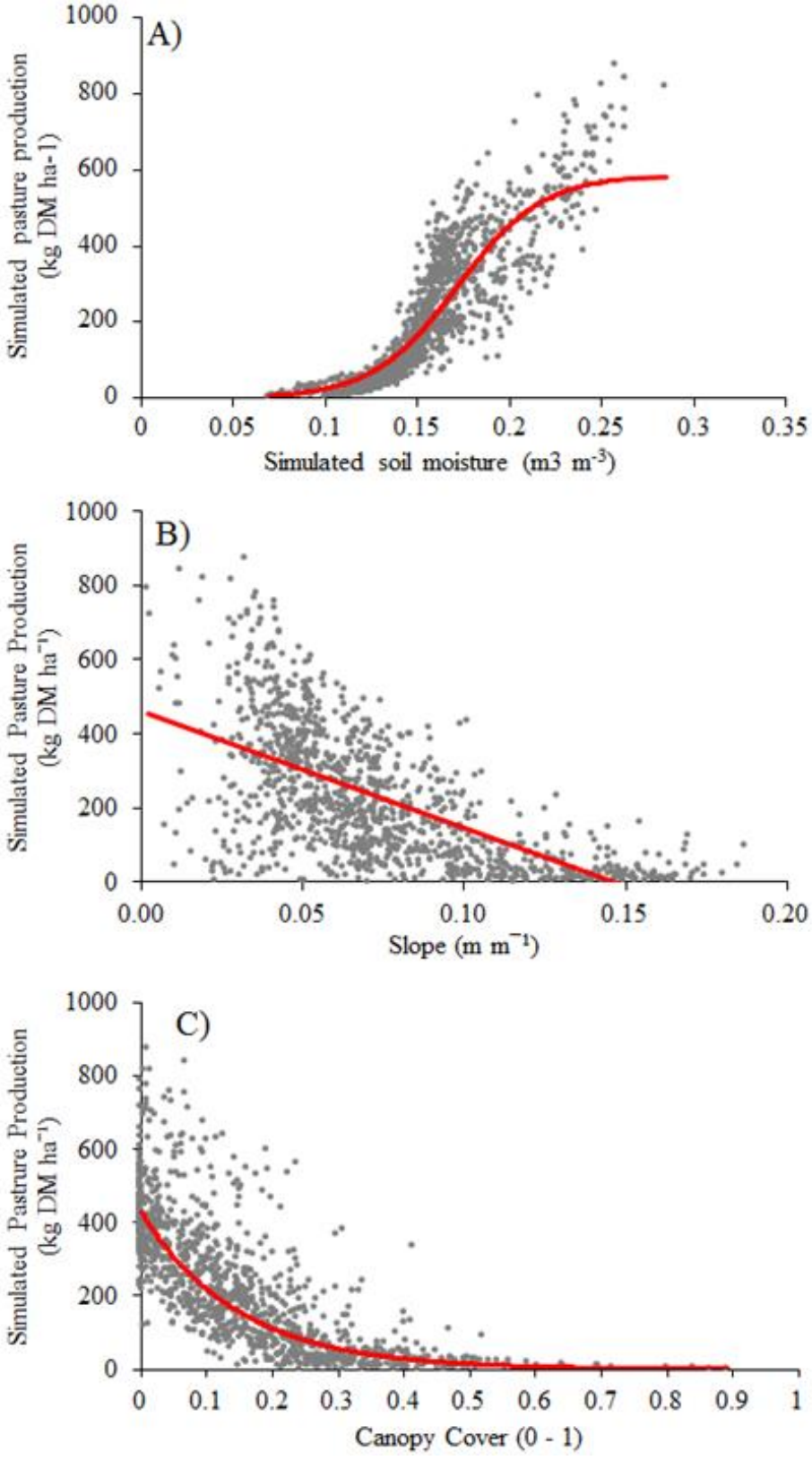

Figure 12. Climate and physiographic factors that influence pasture production